The Arctic is a critical region in the current and past global climate system. One major challenge for investigating the geological history of the Arctic is the establishment of a rigorous chronology. To get better insights into the late Neogene history of oceanographic and climatic change in the region, well-calibrated ocean drill cores are essential. Nevertheless, detailed stratigraphy from (sub)Arctic ocean drill sites remains problematic due to the generally poor preservation of calcareous microfossils in high northern-latitude oceans. Here, organic-walled palynomorphs (dinoflagellate cysts and acritarchs) can compensate for the lack of calcareous microfossils because diverse and rich palynological assemblages can be recovered. We defined three magnetostratigraphically-calibrated dinoflagellate cyst and acritarch biozones in the Upper Miocene to Upper Pliocene of Norwegian Sea Ocean Drilling Program Hole 642B (Vøring Plateau) that show potential for correlation within the Nordic Seas. It is also noted that several bioevents in the Nordic Seas are strongly diachronous with the North Atlantic, highlighting the limitations of applying North Atlantic bioevents directly to the Nordic Seas. For each of the three interval biozones (VP1 to VP3) we use the highest occurrences of acritarch and dinoflagellate cyst species ("*Veriplicidium franklinii*" of Anstey 1992, *Reticulatosphaera actinocoronata*, and *Invertocysta lacrymosa*) that are relatively synchronous across the Nordic Seas and North Atlantic and thus show potential for a North Atlantic–Arctic reference stratigraphy.

Highlights

A new late Neogene marine palynomorph biozonation is presented for the Norwegian Sea

Three biozones covering the uppermost Miocene to Upper Pliocene are defined

The zonation is an important step towards a regional late Neogene Arctic stratigraphy

Correlation between the Nordic Seas and North Atlantic is strongly diachronous

Late Neogene dinoflagellate cyst and acritarch biostratigraphy for Ocean Drilling Program Hole 642B, Norwegian Sea

Stijn De Schepper[1,2], Kristina M. Beck[1], and Gunn Mangerud[1]

[1]Department of Earth Science, University of Bergen, PO Box 7803, N-5020 Bergen, Norway

[2]Uni Research Climate, Bjerknes Centre for Climate Research, Nygårdsgaten 112–114, N-5008 Bergen, Norway

Corresponding author: Stijn De Schepper, smad2@cantab.net, +47 555 83826

Kristina M. Beck, kristina.mar.beck@gmail.com

Gunn Mangerud, Gunn.Mangerud@uib.no, 0047 97557137

Abstract

The Arctic is a critical region in the current and past global climate system. One major challenge for investigating the geological history of the Arctic is the establishment of a rigorous chronology. To get better insights into the late Neogene history of oceanographic and climatic change in the region, well-calibrated ocean drill cores are essential. Nevertheless, detailed stratigraphy from (sub)Arctic ocean drill sites remains problematic due to the generally poor preservation of calcareous microfossils in high northern-latitude oceans. Here, organic-walled palynomorphs (dinoflagellate cysts and acritarchs) can compensate for the lack of calcareous microfossils because diverse and rich palynological assemblages can be recovered. We defined three magnetostratigraphically-calibrated dinoflagellate cyst and acritarch biozones in the Upper Miocene to Upper Pliocene of Norwegian Sea Ocean Drilling Program Hole 642B (Vøring Plateau) that show potential for correlation within the Nordic Seas. It is also noted that several bioevents in the Nordic Seas are strongly diachronous with the North Atlantic, highlighting the limitations of applying North Atlantic bioevents directly to the Nordic Seas. For each of the three interval biozones (VP1 to VP3) we use the highest occurrences of acritarch and dinoflagellate cyst species ("*Veriplicidium franklinii*" of Anstey 1992, *Reticulatosphaera actinocoronata*, and *Invertocysta lacrymosa*) that are relatively synchronous across the Nordic Seas and North Atlantic and thus show potential for a North Atlantic–Arctic reference stratigraphy.

Keywords

47Miocene | Pliocene | palynology | biozones | Nordic Seas | North Atlantic

1 Introduction

The Norwegian Sea links the high-latitude eastern North Atlantic with the Arctic Ocean and is today a critical component of the high-latitude ocean circulation and Arctic climate because of northward heat transport via the Norwegian Atlantic Current. Circulation in the Nordic Seas was different from the present during the earliest Pliocene (Jansen et al., 2000), with a modern-like circulation developing around 4.5 Ma in the Early Pliocene (Knies et al., 2014; De Schepper et al., 2015). In order to gain further understanding of the timing of oceanographic and climatic changes in the Arctic Ocean and Nordic Seas, detailed studies of chronostratigraphically well-calibrated successions are essential (e.g. Mattingsdal et al., 2013). The major challenge for a detailed stratigraphy at (sub)Arctic ocean drill sites remains the poor preservation of calcareous microfossils, or also simply their absence due to the harsh environmental conditions. Calcareous microfossils have not been recorded from the only existing Neogene Arctic Ocean sediment record (ACEX), and establishment of a reference stratigraphy for that region is further hampered by incomplete core recovery and the generally rare presence of organic-walled microfossils (e.g. Moran et al., 2006; Matthiessen et al., 2009a; 2009b). However, recently, at the margin of the Arctic Ocean, on the Yermak Plateau in the Fram Strait, an uppermost Miocene to Quaternary stratigraphic framework for the Atlantic–Arctic gateway was successfully established based on seismic correlation, magnetostratigraphy and biostratigraphy at Ocean Drilling Program (ODP) Sites 910, 911 and 912 (Mattingsdal et al., 2013). Based mainly on palynology and magnetostratigraphy, the base of ODP Hole 911A was placed in the lowermost

Pliocene, with an age likely around 5.2 Ma (Mattingsdal et al., 2013; Grøsfjeld et al., 2014). Schreck et al. (2012) calibrated Neogene dinoflagellate cyst and acritarch bioevents to magnetostratigraphy at Iceland Sea ODP Hole 907A. These bioevents were successfully applied to dating a Central Artic Late Miocene interval (Stein et al., 2016), highlighting the potential of palynology in contributing to dating Arctic and Nordic Seas sediments and establishing an Arctic reference stratigraphy. In the Norwegian Sea, a diverse late Neogene dinoflagellate cyst flora has already been documented by Mudie (1989), but a detailed and up-to-date record of dinoflagellate cyst stratigraphic events is currently required.

In the Nordic Seas, organic-walled palynomorphs (dinoflagellate cysts and acritarchs) can compensate for the absence of calcareous microfossils since their assemblages are known to be diverse, rich and well preserved. Furthermore, our knowledge of late Neogene dinoflagellate cysts and acritarchs has increased steadily since the 1990s following major taxonomic advances and the formal description of numerous new dinoflagellate cyst and acritarch taxa (e.g. Head, 1993, 1996, 1997; Head and Norris, 2003; De Schepper et al., 2004; De Schepper and Head, 2008a, 2014; Schreck et al., 2012; Verhoeven et al., 2014; Versteegh and Zevenboom, 1995). Dinoflagellate cysts have been successfully applied for establishing a detailed late Neogene stratigraphy in the eastern North Atlantic (De Schepper and Head, 2008a, 2009), Iceland Sea (Verhoeven et al., 2011; Schreck et al., 2012) and the North Sea Basin (Louwye et al., 2004; De Schepper et al., 2009; Dybkjær and Piasecki, 2010), suggesting that this should also be achievable in the Norwegian Sea.

Because of the oceanographic and climatic importance of the Norwegian Sea in influencing Arctic climate, we have reinvestigated the palynology of ODP Site 642 with the help of advances in dinoflagellate cyst and acritarch taxonomy. ODP Site 642 (Figure 1) located on the Vøring Plateau is currently influenced by Atlantic waters via the Norwegian Atlantic Current, yet is situated at a latitude comparable to that of the Iceland Sea ODP Site 907, where Schreck et al. (2012) documented Miocene to Pliocene dinoflagellate cyst assemblages. The aim of this study is to establish a new, detailed palynostratigraphy for the Upper Miocene to Pliocene succession in the Norwegian Sea, which may represent a benchmark biozonation that can interlink the North Atlantic, Norwegian Sea, and Arctic Ocean.

2 Materials and methods

2.1 Ocean Drilling Program Hole 642B: lithology and samples

ODP Hole 642B (67°13.5'N, 2°55.7'E; water depth 1268 m, core recovery of 97.5%) located on the outer Vøring Plateau, was drilled with an advanced hydraulic piston corer in 1985 as a part of the ODP Leg 104 (Shipboard Scientific Party, 1987) (Figure 1). The drill hole reached a depth of 221.1 meters below sea floor (mbsf), with a total core recovery of 215.6 m, and penetrated predominantly pelagic to hemipelagic sediments of Holocene through Early Miocene age.

The 40 samples investigated in this study were collected from the lower part of lithological Unit I, Subunit IIA and the upper part of IIB (Figure 2). Unit I (0–65.7

121mbsf) consists of repeated alternations of dark, carbonate-poor glacial mud and
122light, carbonate-rich interglacial sandy mud. Bioturbation and the presence of
123dropstones are common throughout. Subunit IIA (65.7–90.4 mbsf) consists
124predominantly of nannofossil oozes, with minor diatom-nannofossil oozes and
125muds. This subunit is moderately to heavily bioturbated. Subunit IIB (90.4–107.2
126mbsf) consists of siliceous oozes and siliceous muds, one short interval of
127nannofossil ooze and several minor volcanic ash layers, which have been
128moderately to heavily bioturbated.

129## 2.2 *Palynological preparation*

130Samples were first wet sieved at 150 and 63 µm for measurements of
131foraminiferal stable isotopes (Risebrobakken et al., 2015). Consequently, the <63
132µm sediment fraction was dried and processed to extract organic-walled
133palynomorphs at Palynological Laboratory Services Ltd (Holyhead, UK) following
134a slightly modified procedure described in De Schepper and Head (2008b). A
135weighed quantity of each sample (Table 1) was disintegrated and placed into a 1L
136Tripour beaker. One *Lycopodium clavatum* spore tablet (Batch no. 483.216, n =
13718,583 ± 1,708 spores per tablet) was added prior to chemical degradation.
138Calcium carbonate was removed by slowly adding 50% hydrochloric acid (HCl)
139until the sample had stopped reacting. Subsequently, the beaker was topped up
140fully with water, stirred and allowed to settle. The diluted supernatant liquid was
141then sieved through a 10-µm sieve cloth, and the collected residue returned to
142the beaker. To remove silicate, 100 ml of 60% hydrofluoric acid (HF) was added
143and left for two days with periodic stirring. The sample was then topped up with
144water for dilution and the entire residue sieved through a 10-µm sieve cloth and

collected, before it was placed in a 250 ml Pyrex glass. Oxidation was carried out on four samples (642B-9H5, 100–101 cm, 642B-10H2, 40–41 cm, 642B-10H2, 100–101 cm, 642B-10H3, 102–103 cm) before mounting by adding 50% cold nitric acid (HNO_3) to the residue in the beaker (in 25 ml of water) and left for some time, depending on the preservation of the residue present. A short ultrasonic treatment then preceded the sieving as before using water. Before mounting, the residue was mixed with a 1% solution of polyvinyl alcohol (PVA) to prevent clumping, and stained with Safranin-O if necessary. It was then pipetted onto a 32x22 mm cover slip on a low temperature drying plate and allowed to dry. Once dry, the coverslip was mounted onto the glass microscope slide using glycerine jelly optical adhesive.

2.3 Counting, photography and data storage

The focus of this study was the dinoflagellate cyst assemblage, but also acritarchs and terrestrial palynomorphs were identified. At least 250 dinoflagellate cysts were counted in each slide along non-overlapping traverses at 400x magnification using a transmitted light microscope (Zeiss Axiophot and AxioImager.A2). During this regular count, all encountered acritarchs, spores, pollen and fresh water algae were also enumerated. The remainder of the slide was scanned at 200x magnification to identify rare taxa not seen during the regular count. Broken palynomorphs were counted as one unit when more than half of the original form was present.

Photographs of selected dinoflagellate cysts and acritarchs were taken using a Zeiss Axiocam 506 Color on a Zeiss AxioImager.A2 microscope.

All raw data are available at http://doi.pangaea.de/10.1594/PANGAEA.846838.

2.4 *Taxonomy and nomenclature*

Some taxa were grouped due to problematic taxonomy and/or limited stratigraphic value. This includes most *Spiniferites* and *Achomosphaera* species which were lumped as *Spiniferites*/*Achomosphaera* spp. indet. According to Schreck and Matthiessen (2013), the *Batiacasphaera micropapillata* complex comprises both micropapillate and microreticulate forms. Although the distinction is not always easy to make (depending on the quality of the microscope objective), we have classified the purely microreticulate forms as *Batiacasphaera minuta* s.s. *Pyxidinopsis* sp. A has a wall ornament that resembles closely that of *Batiacasphaera sphaerica*, but has a precingular instead of antapical archeopyle. Proximate specimens with low wall ornament comparable to *Batiacasphaera sphaerica*, *Batiacasphaera micropapillata* and *Pyxidinopsis* sp. A where the archeopyle could not unquestionably be determined were assigned to the *Batiacasphaera*/*Pyxidinopsis* spp. indet. group. Reworked dinoflagellate cysts were identified on preservation state and known stratigraphic range outside the uppermost Miocene to Pleistocene.

Nomenclature generally follows De Schepper et al. (2004), De Schepper and Head (2008b, 2014) and Fensome et al. (2008).

2.5 *Age model, errors and sample resolution*

The paleomagnetostratigraphic study of Bleil (1989) reports a complete and apparently continuous sequence of the Bruhnes and Matuyama Chrons, including all major reversals as well as the Gauss/Matuyama boundary. A minor hiatus occurs in the uppermost Gauss Chron (near the 8H and 9H cores boundary), but the Mammoth subchron was positively identified. Also the Gilbert Chron and its

four normal polarity subchrons were identified. The palaeomagnetic reversal ages for ODP Hole 642B reported in Bleil (1989) were recalibrated to the Astronomically Tuned Neogene Time Scale 2012 (ATNTS 2012; Hilgen et al., 2012) (Table 2; see also De Schepper et al., 2015). By linearly correlating the mid-points between two adjacent samples that record a reversal in inclination, we provide an age estimate for each investigated sample and bioevent (Table 3). The error on the palaeomagnetic reversals can amount to half the age difference between the two samples either side of the observed reversal (Weaver and Clement, 1987). The distance between two samples across a magnetic reversal varies from 3 to 41 cm (average 29 cm) in the Pliocene succession of ODP 642, which corresponds to an error of 1.5–21 kyr (average 15 kyr) for the age of the magnetic boundaries.

An accurate age for the samples in core-section 642B-8H6 has not been possible to provide because they lie between a hiatus around 66 mbsf (Bleil, 1989) and the Gauss/Matuyama polarity reversal (2.588 Ma). Sample 642B-8H6, 129–130 cm (65.69 mbsf) is younger than 3.20 Ma, and is certainly older than 2.58 Ma but it may also be older than 3.04 Ma.

Sample spacing varies between 5 and 195 cm, with an average of 84 cm, which corresponds to age intervals of 7 to 257 kyr, with an average of 75 kyr. The sampling resolution has an impact on the accuracy of the estimated ages of a highest occurrence (HO), because the true HO of a species is between the highest sample containing this species and the overlying sample without this species. For ODP Hole 642B, this results in an age for the true HO that can be up to 7(75)257

218kyr younger than the reported age, or older in the case of a lowest occurrence
219(LO).

2203 Results

2213.1 *General*

222Most samples contain mainly well-preserved palynomorph assemblages.
223Exceptions are samples 642B-10H2, 40–41 cm (77.80 mbsf) and 642B-10H3,
224102–103 cm (79.92 mbsf) where counting was hampered by a large amount of
225amorphous material, and sample 642B-11H6, 110–111 cm (94.00 mbsf) where
226preservation was poor and cysts showed some degradation. Dinoflagellate cysts
227and acritarchs dominate the assemblages, but terrestrial palynomorphs (spores
228and pollen) also occur abundantly (Table 1). The fresh water alga *Gelasinicysta*
229*vangeelii* is present in low abundance in most samples.
230The focus of this study was marine palynomorphs, especially the dinoflagellate
231cyst assemblage. The concentration of dinoflagellate cysts is between 376 ± 44
232and 79,854 ± 27,861 dinoflagellate cysts/g dry sediment. A total of 95
233dinoflagellate cyst taxa were recorded in the studied interval and the number of
234dinoflagellate cyst taxa per sample is high at 18(35)53 taxa per sample. Diversity
235(Shannon-Wiener index, Table 1) is highly variable but reveals a gradual
236declining trend towards younger samples. Evenness remained relatively constant
237throughout the studied interval and fluctuates between 0.55–0.78, indicating that
238there is always one taxon (or a few taxa) dominating the samples. Dominant taxa
239in the studied interval include the *Batiacasphaera micropapillata* complex,
240*Habibacysta tectata*, *Nematosphaeropsis labyrinthus*, *Operculodinium*? *eirikianum*
241var. *eirikianum*, cysts of *Protoceratium reticulatum*, round brown cysts and

Spiniferites/*Achomosphaera* spp. The overall assemblage throughout the studied interval contains typical Upper Miocene to Pliocene taxa such as *Achomosphaera andalousiensis* subsp. *andalousiensis*, *Amiculosphaera umbraculum*, *Bitectatodinium raedwaldii*, *Invertocysta lacrymosa*, *Operculodinium tegillatum* and *Pyxidinopsis braboi*, as well as extant taxa (e.g. *Impagidinium aculeatum*, *Lingulodinium machaerophorum*).

Acritarchs constitute a significant part of the marine palynological assemblages, and often outnumber dinoflagellate cysts. The concentration of acritarchs in the studied interval varies between 53 ± 21 and 114,498 ± 39,840 acritarchs/g. A total of 18 acritarch taxa was recorded and the number of acritarch taxa per sample is 1(6)10. The taxa *Cymatiosphaera? invaginata*, *Nannobarbophora walldalei* and small spiny acritarchs dominate the acritarch assemblages, and in the middle Zanclean (after ~4.5 Ma) also *Cymatiosphaera? icenorum* and *Lavradosphaera crista* are abundant.

3.2 Age calibration of selected bioevents

Since a solid palaeomagnetostratigraphy is available for ODP Site 642 (Bleil, 1989), it is possible to provide calibrated ages for the bioevents of individual dinoflagellate cyst and acritarch species following the procedures outlined in De Schepper and Head (2008a) and/or Schreck et al. (2012). Table 3 summarises the calibrated ages for lowest, highest and highest common occurrences in ODP Site 642.

3.3 Biozonation

We have attempted to construct a Nordic Seas biozonation that can serve as a basis for correlation with the North Atlantic and Arctic oceans. Therefore, the zone boundaries have been based on bioevents of species that are relatively synchronous across these regions. Three zones are defined as interval biozones, the body of fossiliferous strata between two specified biohorizons (Figure 2). The several bioevents occurring within these zones can be used for more local-to-regional correlations in the Nordic Seas. Range charts for dinoflagellate cysts and acritarchs are provided in an Appendix.

The biozonation follows the *International Stratigraphic Guide* (abridged version of Murphy and Salvador, 1999). The biozones are given informal names (VP1 to VP3) referring to the location of ODP Site 642 on the Vøring Plateau. The biohorizons used are the HO or LO of dinoflagellate cyst and acritarch taxa. Also, the concepts of highest common occurrence (HCO) and highest persistent occurrence (HPO) (De Schepper and Head, 2008a) are used to describe events within biozones. A HCO is recorded in a sample that marks the highest sample where a particular taxon is noticeably common, but this taxon occurs in lower abundance above the level. A HPO marks the highest sample below which a taxon is persistently recorded (i.e. in successive samples), even if the records consist of few specimens only. The classification of relative abundance of the dinoflagellate cysts and the acritarchs is as follows: *Rare*, 0–2.9 %, *Frequent*, 3–9.9 %, *Common*, 10–29.9%, *Abundant*, 30–49.9 %, and *Dominant* ≥ 50 %.

VP1 Interval biozone

Definition. The body of strata from the base of the studied interval to the HO of "*Veriplicidium franklinii*" of Anstey (1992).

Characteristic events. "*Veriplicidium franklinii*" of Anstey (1992) has a HO in sample 642B-10H7, 30–31 cm (85.20 mbsf) at the top of the zone (Figure 2, Appendix). Additional events characterizing the top of the zone are the HO "*Impagidinium densiverrucosum*" of Zevenboom and Santarelli in Zevenboom (1995), the HPO of *Trinovantedinium glorianum*, and the LOs of *Operculodinium tegillatum* and *Heteraulacacysta* sp. A of Costa and Downie (1979). *Corrudinium devernaliae* has a LO in sample 642B-11H3, 65–66 cm (89.05 mbsf) in the middle of the zone.

Dinoflagellate cyst association. *Nematosphaeropsis labyrinthus*, *Operculodinium centrocarpum* s.s., *Operculodinium*? *eirikianum* var. *eirikianum*, round brown cysts, *Reticulatosphaera actinocoronata*, *Selenopemphix* spp. and *Spiniferites*/*Achomosphaera* spp. indet. are the most abundant taxa. Several heterotrophic taxa (*Barssidinium*, *Lejeunecysta*, *Selenopemphix*) are recorded in every sample in variable abundance (rare to common). The species *Lejeunecysta hatterasensis* is recorded in several samples. *Cerebrocysta poulsenii* and *Selenopemphix armageddonensis* are restricted to this zone only.

Acritarch association. "*Veriplicidium franklinii*" of Anstey (1992) occurs in all samples and is rare to common. Small spiny acritarchs and *Cymatiosphaera*? *invaginata* dominate the acritarch assemblage. *Lavradosphaera crista* is rare to common. *Lavradopshaera canalis*, *Lavradopshaera lucifer*, *Cymatiosphaera*? *aegirii*, *Cymatiosphaera*? *icenorum* and *Nannobarbophora walldalei* are rare and sporadic within the zone.

Reference section. Samples 642B-11H7, 55–56 cm, to 642B-10H7, 30–31 cm (94.95–85.20 mbsf).

Age. Late Messinian to earliest Zanclean, from >5.89 Ma to 5.29 Ma.

Calibration. In ODP Hole 642B, Zone VP1 corresponds to the middle part of the planktonic foraminifer *Neogloboquadrina atlantica* sinistral Zone (Spiegler and Jansen, 1989), the lower radiolarian *Antarctissa whitei* Zone (Goll and Bjørklund, 1989), the upper NN15/NN17 calcareous nannofossil Zone (Donnally, 1989), and the upper PM3 dinoflagellate cyst Zone (Mudie, 1989) (Figure 3).

Correlation. The VP1 Zone (>5.89 Ma to 5.29 Ma) partly overlaps with the *Selenopemphix armageddonensis* Zone (7.6–5.0 Ma) of Dybkjær and Piasecki (2010) (Figure 4), which is defined from the HO of *Hystrichosphaeropsis obscura* to the HO of *Barssidinium evangelineae*. The range of *Selenopemphix armageddonensis* is presumed to correspond approximately to the entire *Selenopemphix armageddonensis* Zone (Dybkjær and Piasecki, 2010). *Hystrichosphaeropsis obscura* and *Barssidinium evangelineae* were not recorded in ODP Hole 642B, but *Selenopemphix armageddonensis* was last recorded in the upper part of the VP1 Zone (sample 642B-11H2, 15–16 cm) (Figure 2).

Comments. Anstey (1992) describes the acritarch "*Veriplicidium franklinii*" from the Upper Miocene through possibly Lower Pliocene of ODP Site 645 (Baffin Bay). Although only known under an informal name, this acritarch appears to have correlation potential across the North Atlantic.

"*Impagidinium densiverrucosum*" of Zevenboom and Santarelli in Zevenboom (1995) is mainly known from the Middle Miocene of The Netherlands and Italy (Zevenboom, 1995) and the Upper Miocene of the Danish North Sea (Dybkjær and Piasecki, 2010) In our study, it has a HO at the top of the VP1 Zone (sample

642B-10H7, 30–31 cm). It is morphologically very distinct, although often broken, and is usually present in low numbers only. Therefore, the HO of the more abundant "*Veriplicidium franklinii*" of Anstey (1992) was chosen as the defining event for the VP1 Zone upper boundary (Figure 2). *Selenopemphix armageddonensis* occurs sporadically in the uppermost Miocene and lowermost Pliocene of the Danish North Sea, and ODP Hole 642B, and was recorded also in the Lower Pliocene of Belgium (Louwye et al., 2004). The LO of *Operculodonium tegillatum* at the top of the zone (Table 2) could be a useful local marker, although it has been reported from the Upper Miocene of the Iceland Sea (Schreck et al., 2012) and the North Sea Basin (Louwye, 1999; Louwye and De Schepper, 2010). Dinoflagellate cysts dominate the marine palynomorph assemblage with an average concentration of 8,202 ± 1,202 cysts/g compared to 5,648 ± 867 acritarchs/g.

VP2 Interval biozone

Definition. The body of strata from the HO of "*Veriplicidium franklinii*" of Anstey (1992) to the HO of *Reticulatosphaera actinocoronata*.

Characteristic events. The top of the zone is defined by the HO of *Reticulatosphaera actinocoronata* in sample 642B-10H2, 40–41 cm. Also the *Batiacasphaera micropapillata* complex, *Selenopemphix brevispinosa* and Cyst type I of de Vernal and Mudie (1989) have their HO in the same sample (Figure 2, Appendix). The range of *Operculodinium tegillatum* corresponds almost to the entire zone: its LO is immediately at the boundary between the VP1 and VP2 Zones, whereas its HO is found in the sample immediately above the zone. The

LOs of *Filisphaera filifera* subsp. *filifera* and *Bitectatodinium raedwaldii* are at the base of the zone in sample 642B-10H6, 65–66 cm (Table 3).

Dinoflagellate cyst association. *Nematosphaeropsis labyrinthus*, *Operculodinium tegillatum*, round brown cysts and *Spiniferites*/*Achomosphaera* spp. are the most abundant taxa. The *Batiacasphaera micropapillata* complex is frequent to abundant. *Operculodinium centrocarpum* s.s. and *Operculodinium*? *eirikianum* var. *eirikianum* are rare to common. *Filisphaera filifera* subsp. *filifera* is frequent in one sample. *Corrudinium*? *labradori* and *Reticulatosphaera actinocoronata* are rare to frequent, and occur in every sample. Cyst type I of de Vernal and Mudie (1989) has an acme in the uppermost part of the zone. Cysts of *Protoceratium reticulatum* (= *Operculodinium centrocarpum* sensu Wall and Dale, 1966) are rare and frequent in the upper two samples of the zone.

Acritarch association. The zone corresponds to an acme of *Cymatiosphaera*? *invaginata* which dominates the acritarch assemblage. Small spiny acritarchs are common. *Cymatiosphaera*? *icenorum*, *Lavradosphaera crista* and *Nannobarbophora walldalei* are rare to frequent throughout the zone. *Lavradosphaera lucifer* has a HO in sample 642B-10H2, 100–101 cm (78.40 mbsf).

Reference section. Samples 642B-10H6, 65–66 cm, to 642B-10H2, 40–41 cm (84.05–77.80 mbsf).

Age. Early Zanclean, 5.18–4.64 Ma.

Calibration. In ODP Hole 642B, Zone VP2 corresponds to the middle to upper part of the planktonic foraminifer *Neogloboquadrina atlantica* sinistral Zone (Spiegler and Jansen, 1989), the upper *Antarctissa whitei* radiolarian Zone (Goll and Bjørklund, 1989), and the uppermost NN15/NN17 calcareous nannofossil

zone (Donnally, 1989) (Figure 3). The upper boundary of the VP2 Zone coincides with the upper boundary of the *Antarctissa whitei* radiolarian Zone and NN15/NN17 calcareous nannofossil Zone. This zone has no equivalent in the dinoflagellate cyst zonation, as this interval was left unstudied by Mudie (1989).

Correlation. In the Nordic Seas, the *Batiacasphaera micropapillata* complex (including *Batiacasphaera minuta*) has a HO in the sample below the HOs of *Corrudinium devernaliae* and *Operculodinium tegillatum*. In the North Atlantic, the RT1, RT2 and RT3 zones (~4.0–3.71 Ma) are defined respectively by the HOs of *Corrudinium devernaliae* (top RT1), *Batiacasphaera minuta* (top RT2) and *Operculodinium tegillatum* (top RT3). The sequential order of the HOs is different between both regions making a detailed correlation between the North Atlantic and Nordic Seas biozones difficult. Based on the occurrence of the same marker dinoflagellate cyst species, the RT1, RT2 and RT3 biozones (~4.0–3.71 Ma) can be correlated to the upper VP2 Zone (5.18–4.64 Ma), but the correlation is strongly asynchronous (Figure 4). The upper VP2 Zone correlates to the lower *Melitasphaeridium choanophorum* Zone (5.0–3.60 Ma) of Dybkjær and Piasecki (2010).

Comments. Our study presents a refinement of the stratigraphic ranges of *Reticulatosphaera actinocoronata* and *Filisphaera filifera* subsp. *filifera* at ODP Hole 642B. Mudie (1989) recorded the HO of *Reticulatosphaera actinocoronata* in Hole 642B, sample 642B-14CC, 20 cm (120.10 mbsf), but we document the HO of *Reticulatosphaera actinocoronata* in sample 642B-10H2, 40–41 cm (77.80 mbsf, 4094.64 Ma), with five higher occurrences being interpreted as reworked. We consider the specimens of *Reticulatosphaera actinocoronata* recorded above 177.80 mbsf to be reworked based on the observations that (1) these are either

single occurrences or occurrences recorded outside the regular count, (2) in the same samples single occurrences of other Lower Pliocene species are recorded (e.g. *Batiacasphaera micropapillata* complex, *Operculodinium tegillatum* in samples at 68.3, 70.45 mbsf), or (3) they co-occur with a large amount of undifferentiated reworked specimens (n=134 reworked cysts in sample 65.34 mbsf). Mudie (1989) also reported *Reticulatosphaera actinocoronata* from Hole 642C, where it has a HPO in sample 642C-11H3, 56–57 cm (76.56 mbsf) at ~4.4 Ma (based on linear interpolation between the palaeomagnetic reversal for the hole by Bleil (1989), updated to ATNTS2012 of Hilgen et al., 2012). Our new observations place the range top of this species in Hole 642B closely to its range top in Hole 642C.

Mudie (1989) placed the LO of *Filisphaera filifera* in sample ODP 642B-9CC, 18 cm (76.25 mbsf) considerably higher than our observation of its LO in sample 642B-10H6, 65–66 cm (84.05 mbsf). We even recorded a single specimen of *Filisphaera filifera* subsp. *pilosa* in the underlying VP1 Zone in sample 642B-11H3, 65–66 cm (89.05 mbsf). The difference between our observations and those of Mudie (1989) can be explained by the lower sampling resolution of 1 sample per 9 m in this part of the section (see discussion).

Cyst type I of de Vernal and Mudie (1989) occurs between 4.81 to 4.64 Ma (Table 3), with a clear acme between 4.69 and 4.64 Ma. This record corresponds to other Zanclean records in the Labrador Sea (ODP Hole 646B), western North Atlantic (DSDP Hole 603C), and off West Greenland (M.J. Head, pers. comm. in Louwye et al., 2004; Piasecki, 2003). In DSDP Hole 603C, this species has a restricted range between 4.66 and 4.21 Ma, with an acme between 4.54 and 4.32 Ma (M.J. Head, unpublished data).

Average dinoflagellate cysts concentrations (34,331 ± 9392 cysts/g) are considerably higher than the VP1 Zone, but acritarchs are the dominant marine palynomorph group with an average concentration of 40,698 ± 11,050 acritarchs/g.

VP3 Interval biozone

Definition. The body of strata from the HO of *Reticulatosphaera actinocoronata* to the HO of *Invertocysta lacrymosa*.

Characteristic events. At the base of the zone, *Corrudinium devernaliae* and *Operculodinium tegillatum* have their HOs in sample 642B-10H1, 145–146 cm (77.35 mbsf). The ranges of *Ataxiodinium confusum*, *Operculodinium*? *eirikianum* var. *crebrum*, *Impagidinium solidum*, *Melitasphaeridium* sp. A of De Schepper and Head (2008b) and *Spiniferites elongatus* are restricted to this zone (Figure 2, Appendix). At or just below the top of this zone, the HOs of *Bitectatodinium*? *serratum*, *Melitasphaeridium choanophorum*, *Ataxiodinium zevenboomii*, *Corrudinium*? *labradori*, *Heteraulacacysta* sp. A of Costa and Downie (1979), *Operculodinium janduchenei*, *Trinovantedinium glorianum* and *Achomosphaera andalousiensis suttonensis* are recorded.

Dinoflagellate cyst association. *Filisphaera filifera*, *Nematosphaeropsis labyrinthus*, cysts of *Protoceratium reticulatum*, and *Spiniferites*/*Achomosphaera* spp. are the most abundant taxa. The relative abundance of cysts of *Protoceratium reticulatum* increases sharply across the lower boundary of the zone to reach at least 25% in most samples of this biozone, except the uppermost sample which is dominated by *Habibacysta tectata* and *Filisphaera filifera* subsp. *filifera*. *Operculodinium*? *eirikianum* var. *eirikianum* is less abundant than in Zone

VP2. *Corrudinium*? *labradori* (rare), *Impagidinium pallidum* (rare to frequent), *Impagidinium aculeatum* (rare) and *Impagidinium paradoxum* (rare) are consistently present.

Acritarch association. Acritarchs are very abundant in this zone and outnumber the dinoflagellate cysts in the lower and middle part of the zone, except in the lowermost sample which yielded very few acritarchs (Table 1). The assemblages are dominated by small spiny acritarchs. *Lavradosphaera crista* is generally common to frequent, and shows a decline in the upper part of the zone when dinoflagellate cysts become more abundant. *Lavradosphaera crista* has a HCO/HPO in sample 642B-9H1, 120–121 cm (67.60 mbsf). *Cymatiosphaera*? *invaginata* is abundant throughout the zone. *Cymatiosphaera*? *icenorum* has a well-expressed acme between samples 642B-10H1, 40–41 cm (76.30 mbsf) and 642B-9H2, 110–111 cm (69.00 mbsf).

Reference section. Samples 642B-10H1, 145–146 cm, to 642B-9H1, 120–121 cm (77.35–67.60 mbsf).

Age. Zanclean to Piacenzian, between 4.49 to 3.27 Ma.

Calibration. In ODP Hole 642B, Zone VP3 corresponds to the uppermost part of the planktonic foraminifer *Neogloboquadrina atlantica* sinistral Zone (Spiegler and Jansen, 1989), and the upper boundary of both zones seems to coincide (Figure 3). Zone VP3 corresponds to the *Pseudodictyophimus gracilipes tetracanthus* radiolarian Zone (Goll and Bjørklund, 1989), the lowermost NN16/NN19 calcareous nannofossil Zone (Donnally, 1989), and the lowermost PM2 dinoflagellate cyst Zone (Mudie, 1989).

Correlation. Apparently diachronous (see section 4.3), the upper *Melitasphaeridium choanophorum* Zone (5.0–3.60 Ma, Dybkjær and Piasecki,

2010) corresponds to the VP3 Zone (Figure 4). The VP3 Zone further correlates to the North Atlantic RT4 (3.71–3.15 Ma) and RT5 (3.15–2.74 Ma) Zones, but reveals a strong diachroneity.

Comments. Acritarchs are the dominant palynomorph group within the zone with an average concentration of 10,888 ± 1,534 acritarchs/g. Dinoflagellate cysts occur with an average of 6,100 ± 919 cysts/g.

NOT ZONED

The four samples in the interval between 66.90 and 64.54 mbsf (642B-9H1, 50–51 cm to 642B-8H6, 14–15 cm) are difficult to date and we have not established a zone, due to a hiatus near the 8H and 9H cores boundary (~66 mbsf; Bleil, 1989). In the second sample below the hiatus, several dinoflagellate cyst species as well as the acritarch *Lavradosphaera crista* disappear from the record. These HOs are part of the clear decrease in diversity that is visible in the upper part of the studied interval (Table 1). Several of the species recorded in the not zoned interval (e.g. *Barssidinium* spp., *Filisphaera filifera* subsp. *filifera*, *Habibacysta tectata*, *Amiculosphaera umbraculum*) disappear from the North Atlantic record during the Pleistocene (De Schepper and Head, 2009).

4 Discussion

4.1 Comparison with the ODP Hole 642B palynological study by Mudie (1989)

Assisted by considerable advances in dinoflagellate cyst and acritarch taxonomy since the mid-1990s, we have recorded 95 dinoflagellate cyst taxa and 18 acritarch taxa in the Pliocene of ODP Hole 642B compared to 52 dinoflagellate cyst and 3 acritarch taxa in Mudie (1989). Only 19 taxa are in common with the

study of Mudie (1989), however this number does not take into account the several taxa left in open nomenclature by Mudie (1989).

The sampling resolution of our study is considerably higher than that of Mudie (1989), and was more focused on the Miocene–Pliocene. We analysed 40 samples from the Pliocene–Miocene interval in ODP 642B from core-section 642B-8H6 to 642B-11H7 with a sample interval from 5 to 195 cm (~5,000 to ~200,000 years). In comparison, Mudie (1989) investigated the entire Quaternary to Miocene section with a 1 m sample resolution down to core 642B-8H6 and every core catcher (~9 m) between 642B-9H to 642B-20H (i.e. the Pliocene–Miocene interval).

The three zones (VP1, VP2, VP3) defined in the present study compare to the PM zones of Mudie (1989) as follows (Figure 3): Zone VP1 corresponds to the uppermost part of Zone PM3 and our youngest Zone VP3 corresponds to the lowermost part of Zone PM2. The top of zone PM3, thought to be roughly corresponding to the Miocene–Pliocene boundary, was defined at the HCO of *Amiculosphaera umbraculum* (Mudie, 1989). We identified, however, this species throughout the studied interval, with its highest abundance near the top of the studied interval. *Amiculosphaera umbraculum* is known also from the Pleistocene eastern North Atlantic up to 1.44 Ma (De Schepper and Head, 2008a) and can therefore not be used as a stratigraphic marker for the Miocene–Pliocene transition. Nevertheless, by coincidence, the upper boundary of our VP1 Zone corresponds to the upper boundary of the PM3 Zone.

Mudie (1989) recorded the LO of *Tectatodinium pellitum* and *Filisphaera filifera* (642B-9H-CC, 18 cm) at the base of zone PM2 although one occurrence of *Filisphaera filifera* below in sample 642B-12-CC, 28 cm is shown (Fig. 5 in Mudie, 1989). It must be pointed out that the illustrated specimen of *Tectatodinium*? sp. of Piasecki (1980) (pl. 5, fig. 2 in Mudie, 1989) is in fact *Tectatodinium pellitum*, whereas the illustrated *Tectatodinium pellitum* (pl. 5, figs. 1, 5 in Mudie, 1989) is likely a different taxon. This could be the result of mislabeling the plates or reflect taxonomical issues. In the present study, *Tectatodinium pellitum* was recorded throughout the study interval. We identified the LO of *Filisphaera filifera* subsp. *filifera* in sample 642B-10H6, 65–66 cm, at the base of our VP2 Zone. Note that our VP2 Zone was identified in an interval of the core that was left unstudied by Mudie (1989) (Figure 3).

4.2 *Correlations with and implications for the (Pliocene) Danish North Sea zonation of Dybkjær and Piasecki (2010)*

In Denmark, a Neogene dinoflagellate cyst biozonation was established from a combination of onshore and offshore well sections (Dybkjær and Piasecki, 2010). Due to the absence of sections with reliable marine isotope stratigraphy or magnetostratigraphy within the Danish North Sea, the ages assigned to the different Danish biozones were obtained from other locations where calibrated sections are available and/or from data compilations (Powell and Brinkhuis in Lourens et al. 2005). The identification of index species in the Danish Neogene North Sea sediments allowed the biozones to be correlated to the western North Atlantic zonation of de Verteuil and Norris (1996). The Danish North Sea

Selenopemphix armageddonensis and *Melitasphaeridium choanophorum* biozones can also be recognised in the Norwegian Sea, where they broadly correspond to the VP1–VP2 and VP2–VP3 zones respectively (Figure 4).

The Upper Miocene to lowermost Pliocene *Selenopemphix armageddonensis* Zone (7.6–5.0 Ma) in the Danish North Sea is defined between the HO of *Hystrichosphaeropsis obscura* and the HO of *Barssidinium evangelineae* (Dybkjær and Piasecki, 2010). The range of *Selenopemphix armageddonensis* is presumed to approximate the range of the zone (Dybkjær and Piasecki, 2010). Specimens of *Selenopemphix armageddonensis* were identified in three samples of our VP1 Zone, suggesting at least a partial overlap of the VP1 Zone with the *Selenopemphix armageddonensis* Zone. However, *Barssidinium evangelineae* was not identified in ODP Hole 642B.

Although sometimes problematic due to the occurrence of reworked specimens in Upper Pliocene sediments, a generally good index species for correlating Lower Pliocene deposits between the Norwegian Sea and Danish North Sea is *Reticulatosphaera actinocoronata*. This species has its LO within the *Melitasphaeridium choanophorum* Zone in the Danish North Sea (Dybkjær and Piasecki, 2010) and defines the top of our VP2 Zone. It has a relatively well-established HO in several North Atlantic locations at 4.4–4.5 Ma (Louwye et al., 2004; Schreck et al., 2012) adding value to its use as an index fossil. Using the HO of *Reticulatosphaera actinocoronata* to subdivide the *Melitasphaeridium choanophorum* Zone in the Danish North Sea could further refine the dinoflagellate cyst biozonation there.

585

586The top of the *Melitasphaeridium choanophorum* Zone (Dybkjær and Piasecki,
5872010) is characterised by the HO of *Melitasphaeridium choanophorum* which
588occurs ~3.6 Ma according to the data compilation of Powell and Brinkhuis in
589Lourens et al. (2005). In contrast, this species is recorded in the VP3 Zone until
590~3.3 Ma in the Norwegian Sea and has a HPO around 3.0 Ma in the North
591Atlantic, where also occasional occurrences are recorded in the Pleistocene
592(Head and Westphal, 1999; De Schepper and Head, 2009). In fact, this species is
593recorded in modern sediments of the Gulf of Mexico, which may act as a refuge
594for this warm-water species today (Limoges et al., 2013). It is thus clear that the
595HO of *Melitasphaeridium choanophorum* is diachronous, and an age of 3.6 Ma – as
596listed in the compilation of Powell and Brinkhuis in Lourens et al. (2005) – for
597the upper boundary of the *Melitasphaeridium choanophorum* Zone in the Danish
598Basin is probably too old. Especially since it occurs in younger deposits in the
599Norwegian Sea (this study), North Atlantic (De Schepper and Head, 2009) and
600the southern North Sea Basin (Louwye et al., 2004; De Schepper et al., 2009). In
601addition, the HOs of *Invertocysta lacrymosa* and *Barssidinium graminosum* occur
602just above the HO of *Melitasphaeridium choanophorum* in the Danish North Sea
603(Dybkjær and Piasecki, 2010). Both *Invertocysta lacrymosa* and *Barssidinium*
604*graminosum* have a last appearance at 2.74 Ma, about 250,000 years after the last
605appearance of *Melitasphaeridium choanophorum* in the eastern North Atlantic
606(De Schepper and Head, 2008a; 2009). Also at the Vøring Plateau both species
607occur well into the Upper Pliocene (this study). Together, this suggests a Late
608Pliocene age for the top of the Danish Basin *Melitasphaeridium choanophorum*

Zone rather than an Early Pliocene age proposed by Dybkjær and Piasecki (2010).

4.3 Correlations with the Iceland Sea and North Atlantic

4.3.1 Upper Miocene correlations

There are only few sections available for comparison that cover the Upper Miocene to Pliocene in the North Atlantic realm, and these often only have limited age control (e.g. Labrador Sea ODP Site 646; de Vernal and Mudie, 1989). Eastern North Atlantic DSDP Hole 610A has a calibrated dinoflagellate cyst zonation that covers the Lower Pliocene from ca. 4 Ma onwards to Pleistocene (Figure 4) (De Schepper and Head, 2009). In Iceland Sea ODP Hole 907A, Schreck et al. (2012) recorded stratigraphically-calibrated ranges of selected dinoflagellate cyst species for the Miocene to Pliocene, but a biozonation was not established.

Correlations of the uppermost Miocene at ODP Site 642 with the Iceland Sea and North Atlantic are hampered by the limited availability of marker species for this time interval (e.g. Schreck et al., 2012). For example, *Cristadinium cristatoserratum* (HO at 8.3 Ma) and the acritarch *Decahedrella martinheadii* (HO 6.5 Ma) are two of the Upper Miocene markers of Iceland Sea ODP Hole 907A (Schreck et al., 2012), but these events are older than the studied section at ODP Hole 642B.

4.3.2 Lower Pliocene correlations

The HO of *Reticulatosphaera actinocoronata* likely presents the best correlative marker within the Nordic Seas and with the wider North Atlantic region in the

633Lower Pliocene. The last appearance in the Norwegian Sea at 4.64 Ma and in the
634Iceland Sea at 4.45 Ma correspond favourably to the relatively well-established
635last appearance in several North Atlantic locations at around 4.4–4.5 Ma (reviews
636in Louwye et al., 2004; Schreck et al., 2012). The HO of *Reticulatosphaera*
637*actinocoronata* could therefore be used in the future for a Neogene North Atlantic
638– Nordic Seas reference stratigraphy.
639
640Applying the eastern North Atlantic zonation of De Schepper and Head (2009) to
641the Vøring Plateau is problematic due to the difference in stratigraphic ranges of
642the marker species. Whereas several Early Pliocene bioevents and biozones are
643near-synchronous between the Norwegian Sea and Iceland Sea, these are
644strongly diachronous compared to the North Atlantic (Figure 4). The Lower
645Pliocene North Atlantic RT1 to RT3 zones correlate to the uppermost VP2 and
646lowermost VP3 zones, but this correlation is strongly diachronous. The
647sequential disappearance of *Corrudinium devernaliae* (3.90 Ma), *Batiacasphaera*
648*micropapillata* complex (3.83 Ma) and *Operculodinium tegillatum* (3.71 Ma),
649which characterise the upper boundaries of respectively the North Atlantic RT1,
650RT2 and RT3 zones, is not observed in the Nordic Seas (Figure 4). Instead, in ODP
651Hole 642B, the HOs of *Operculodinium tegillatum* and *Corrudinium devernaliae*
652are observed in one sample (4.49 Ma) immediately above the HO of the
653*Batiacasphaera micropapillata* complex (4.64 Ma). Also, all three species have
654their HO (or HPO) in the Early Pliocene of Iceland Sea ODP Site 907 between
6554.45–4.55 Ma (Schreck et al., 2012). Thus, the HOs of *Corrudinium devernaliae*,
656*Batiacasphaera micropapillata* complex and *Operculodinium tegillatum* are
657recorded at least 500,000 years later in the North Atlantic than in the Iceland and

Norwegian seas. This discrepancy in timing of the bioevents between both basins can likely be attributed to the first development of the modern ocean circulation in the Nordic Seas around 4.5 Ma (De Schepper et al., 2015). The contemporaneous extinction events and major overturn in the phytoplankton assemblages across the Nordic Seas, suggest a cooling throughout the Nordic Seas followed by the development of a proto-East Greenland Current and Norwegian Atlantic Current.

Correlation of the North Atlantic RT4 Zone (De Schepper and Head, 2009) to the Norwegian Sea appears similarly problematic. The RT4 Zone is the interval between the HO of *Operculodinium tegillatum* and the HO of *Impagidinium solidum* in DSDP Hole 610A and straddles the Early–Late Pliocene boundary. In the Nordic Seas, it is not practical to define a biozone using the HOs of these two species. Firstly, we already established that the HO of *Operculodinium tegillatum* is recorded up to 800,000 years earlier in the Norwegian Sea than in the North Atlantic. Secondly, *Impagidinium solidum* occurs rarely in ODP Hole 642B between 3.83 and 3.59 Ma and this may not represent its total stratigraphic range. If the record at 3.59 Ma does represent its HO, then the HO of *Impagidinium solidum* is also recorded 500,000 years earlier in the Norwegian Sea (3.59 Ma) than in the North Atlantic (3.15 Ma). Since *Impagidinium solidum* has a preference for warm waters (De Schepper et al., 2011), its presence in the Nordic Seas may be restricted to the Early Pliocene, whereas it can persist longer in the warmer, more southerly eastern North Atlantic.

4.3.3 Upper Pliocene correlations

The stratigraphic ranges of Upper Pliocene dinoflagellate cysts are also strongly diachronous between the Nordic Seas and North Atlantic. For example, *Melitasphaeridium* sp. A of De Schepper and Head (2008b) and *Operculodinium*? *eirikianum* var. *crebrum* have overlapping ranges near the Early–Late Pliocene boundary in the Norwegian Sea (3.6–3.5 Ma). Such overlap is also encountered in the North Atlantic, yet this occurs considerably later around ca. 3.2 Ma (De Schepper and Head, 2008a). This observation demonstrates also a diachroneity between the North Atlantic and Norwegian Sea bioevents in the Late Pliocene.

A Late Pliocene major extinction event is recognised in the Norwegian Sea around 3.3 Ma when four dinoflagellate cysts (*Heteraulacacysta* sp. A of Costa and Downie (1979), *Invertocysta lacrymosa*, *Operculodinium janduchenei* and *Melitasphaeridium choanophorum*) and one acritarch (*Lavradosphaera crista*) disappear simultaneously (Figure 2, 4, Appendix). Their disappearance from ODP Hole 642B at 67.60 mbsf is not related to the hiatus in the upper part of the Gauss Chron of ODP Hole 642B which occurs higher around 66 mbsf (Bleil, 1989). These HOs, dated at 3.27 Ma, could be related to a major Northern Hemisphere cooling event during MIS M2 (ca. 3.3 Ma; De Schepper et al., 2013). However, after MIS M2 sea surface temperatures remain fluctuating between 0 and 3 ˚C above Holocene values (Bachem et al. 2016), suggesting that high latitude cooling may not be the only cause of their disappearance. Irrespective of what is causing the HOs, a strong asynchrony remains apparent with their HOs in the North Atlantic (Figure 4), where these species range into younger Late Pliocene sediments (< 3 Ma). It is thus possible to recognise the North Atlantic

RT5 zone, defined between the HO of *Impagidinium solidum* (but see earlier comments on its range) and HO of *Invertocysta lacrymosa*, in the Norwegian Sea where it corresponds to the upper VP3 Zone (Figure 3, 4). But also here, there is strong diachroneity between the different zones (RT5 Zone, 3.15–2.74 Ma vs. VP3 Zone, 4.49–3.27 Ma), which could be related to deteriorating climate associated with the onset of the Northern Hemisphere glaciation and/or the hiatus in the Norwegian Sea record. These species are not recorded from the Iceland Sea where the Late Pliocene sediments are generally barren (Schreck et al., 2012).

5 Conclusions

Three dinoflagellate cyst interval biozones (VP1, VP2, VP3) are established for the latest Miocene to Late Pliocene of Vøring Plateau ODP Hole 642B using the most up-to-date taxonomy and a higher resolution compared to the pioneering work of Mudie (1989). The zones and stratigraphic ranges of selected dinoflagellate cysts and acritarchs are calibrated to the available magnetostratigraphy (Bleil, 1989). The oldest Zone VP1 corresponds to the late Messinian–earliest Zanclean, Zone VP2 is restricted to the early Zanclean and the youngest Zone VP3 covers the late Zanclean to middle Piacenzian. Some of the Upper Miocene Arctic (e.g. *Decahedrella martinheadii*) and North Atlantic (e.g. *Barssidinium evangelineae*) marker species were missing from our studied interval in ODP Hole 642B, hampering correlations with the Upper Miocene biozones from the Iceland Sea and Danish Basins. The HOs of the dinoflagellate cyst species *Reticulatosphaera actinocoronata* and *Invertocysta lacrymosa* were used to define the upper boundaries of the VP2 Zone, and the upper boundary of the VP3 Zone, respectively. These two Pliocene bioevents seem to be relatively

731synchronous between the Nordic Seas and North Atlantic and may serve as the
732basis for a future Pliocene North Atlantic–Arctic reference stratigraphy.
733
734Our dinoflagellate cyst biozonation for the Vøring Plateau ODP Hole 642B has
735potential to be a benchmark for linking Arctic and North Atlantic zonations and
736for dating and correlating late Neogene deposits along the Norwegian Shelf. The
737Early Pliocene Norwegian Sea bioevents (disappearances of *Reticulatosphaera*
738*actinocoronata*, *Operculodinium tegillatum*, *Corrudinium devernaliae*,
739*Batiacasphaera micropapillata* complex) are observed in contemporaneous
740Iceland Sea sediments, but these Nordic Seas events are strongly asynchronous
741with the North Atlantic. Late Pliocene Norwegian Sea HO (e.g. HOs of
742*Ataxiodinium confusum*, *Operculodinium*? *eirikianum* var. *crebrum*,
743*Melitasphaeridium choanophorum*) are also asynchronous with the North
744Atlantic, demonstrating that several events are only useful for local to regional
745correlations. Because of the diachronous ranges of several species in the different
746basins, it is clear that one must apply North Atlantic biozonation schemes with
747caution in the Nordic Seas (e.g. Anthonissen, 2009) or if applying the Nordic Seas
748biozonation into the North Atlantic and North Sea. To improve inter-basin
749correlations, a well-calibrated, continuous upper Neogene record in the southern
750Norwegian Sea – northern North Sea region would be a major asset in tying the
751North Atlantic and Norwegian biozonations together.
752
753Finally, while we focused on the Late Miocene and Pliocene, it would be valuable
754to re-investigate Early and Middle Miocene marine palynology (Manum et al.,
7551989) applying the modern taxonomic concepts and biozonation schemes

available (de Verteuil and Norris, 1996; Munsterman and Brinkhuis, 2004; Dybkjær and Piasecki, 2010) to improve understanding of Neogene oceanographic and climate evolution of the Arctic region.

Taxonomic appendix

"*Veriplicidium franklinii*" of Anstey (1992): This thin-walled, autophragmal palynomorph with scabrate to finely granulate wall was first described in an unpublished MSc thesis (Anstey, 1992). The vesicle appears elongate, likely due to the typical occurrence of several mainly longitudinal folds of the autophragm. On our specimens, an excystment aperture was not observed, but Anstey (1992) reports an angular rupture-type aperture in the apical region based on SEM analysis. Measurements based on 8 specimens: vesicle length, 27[32]34 µm; width, 19[21]23 µm. These compare well with the dimensions reported by Anstey (1992): length, 27[32]38 µm; width, 10[24]27 µm.

Batiacasphaera micropapillata complex and *Batiacasphaera minuta* s.s.: We follow the concept of Schreck and Matthiessen (2013) which groups all (sub)spherical, transparent specimens bearing an apical archeopyle and a microreticulate, vermiculoreticulate–vermiculate and rugulate ornamentation. Our *Batiacasphaera micropapillata* complex likely includes specimens that can be attributed to the exclusively microreticulate *Batiacasphaera minuta* s.s. (e. g. in sample 642B-10H5, 115–116 cm; 642B-10H5, 11–12 cm), but when *Batiacasphaera minuta* s.s. was unequivocally recognised, it was categorised as such.

Batiacasphaera/Pyxidinopsis spp. indet.: This group contains all (sub)spherical, transparent cysts bearing a low wall ornament (granulate, punctate to

punctoreticulate) of which the archeopyle (precingular or apical?) could not clearly be determined.

Bitectatodinium sp. A: (Sub)spherical cysts bearing a precingular (2P) archeopyle as for the genus *Bitectatodinium*. This species has a wall ornament that is intermediate between the typical vermiculate ornament of *Bitectatodinium tepikiense* and the "hairy" ornament of *Bitectatodinium raedwaldii*. The wall ornament of *Bitectatodinium* sp. A is a dense pattern of pili (as for *B. raedwaldii* Head, 1997) and short, straight (as for *B. tepikiense* Wilson, 1973) or irregular polygonal ridges. This pattern is best observed using L-O (Lux-Obscura) analysis at 1000x magnification. *Bitectatodinium* sp. A is here considered to have a transitional morphology between the end-members *Bitectatodinium raedwaldii* and *Bitectatodinium tepikiense*, and is therefore left in open nomenclature.

"Impagidinium densiverrucosum" Zevenboom and Santarelli in Zevenboom (1995): Rare but distinct large, (sub)spherical cyst with a dense and coarse verrucate wall ornament on all plates. Relatively high and smooth crests appear to delineate tabulation, likely of an *Impagidinium*. The encountered specimens are often broken. Measurements based on 5 specimens: maximum inner diameter, 66[78]88 µm; crest height, 3[3.3]3.5 µm. Diameter measurements should be treated with care since 4 specimens were broken and one was folded. This taxon was listed as *Impagidinium vermiculatum* by Beck (2013).

Cysts of *Protoceratium reticulatum*: Paez-Reyes and Head (2013) proposed this name for specimens of *Operculodinium centrocarpum* sensu Wall and Dale, 1966. Both forms with short and long processes are included here.

Pyxidinopsis sp. A: (Sub)spherical transparent cysts with apical archeopyle, bearing a low wall ornament that is granulate, punctate to punctoreticulate. This taxon closely resembles *Batiacasphaera sphaerica* except for the archeopyle which is precingular. When the archeopyle was not fully visible, specimens were generally grouped under *Batiacasphaera*/*Pyxidinopsis* spp. indet., however it is possible that some specimens of *Batiacasphaera sphaerica* may have been classified as *Pyxidinopsis* sp. A.

Cyst type I of de Vernal and Mudie (1989): spherical palynomorph, possibly a dinoflagellate cyst with an apical archeopyle. Numerous thin solid, straight and bent processes end distally in broad, ornamented trabeculae. Trabeculae delimit large (4–6 µm diameter) and occasional small (2 µm diameter) circular to oval openings. Large excystment aperture (apical archeopyle?), operculum free.

Lavradosphaera? sp.: Questionably assigned to the genus *Lavradosphaera* due to the very reduced cancellous wall, which consist of solitary thin rods that support the outer wall on these specimens.

Lavradosphaera sp. cf. *canalis*: Spherical cyst bearing U-shaped channels typical of *Lavradosphaera canalis*. The specimens are assigned questionably to the species because the typical cancellous wall structure for the genus

Lavradosphaera is very reduced, and appears to consist of several, solitary thin rods supporting the outer wall.

Acknowledgements

This work is based on the MSc thesis of Kristina Beck (University of Bergen, Norway). Malcolm J. Jones of Palynological Laboratory Services Ltd, Holyhead (UK) is thanked for the palynological preparations. Funding for sample preparations from Statoil ASA is appreciated. The Integrated Ocean Drilling Program provided the samples. B. Risebrobakken is thanked for making the samples available (Norwegian Research Council project 221712). SDS acknowledges funding from the Norwegian Research Council (project 229819). We are grateful for the constructive comments of K. Dybkjær and M.J. Head.

References

Anthonissen, E.D., 2009. A new Pliocene biostratigraphy for the northeastern North Atlantic. Newsl. Stratigr. 43, 91–126.

Anstey, C. E., 1992. Biostratigraphic and paleoenvironmental interpretation of upper middle Miocene through lower Pleistocene dinoflagellate cyst, acritarch, and other algal palynomorph assemblages from Ocean Drilling Program Leg 105, Site 645, Baffin Bay. Unpubl. MSc thesis, University of Toronto, Canada, pp. 1–257.

Bachem, P.E., Risebrobakken, B., McClymont, E.L., 2016. Sea surface temperature variability in the Norwegian Sea during the late Pliocene linked to subpolar gyre strength and radiative forcing. Earth Planet. Sci. Lett. 446, 113–122.

Beck, K.M., 2013. Latest Miocene to Late Pliocene Dinoflagellate Cyst Biostratigraphy of the Ocean Drilling Program Hole 642B on the Vøring Plateau. Unpubl. MSc thesis, University of Bergen, Norway, pp. 1–92, http://bora.uib.no/handle/1956/8413

Bleil, U., 1989. Magnetostratigraphy of Neogene and Quaternary sediments series from the Norwegian Sea: Ocean Drilling Program, Leg 104. Proc. ODP Sci. Res. 104, 829–901.

Costa, L., Downie, C., 1979. Cenozoic dinocyst stratigraphy of Sites 403 to 406 (Rockall Plateau), IPOD, Leg 48. DSDP Init. Rep. 48, 513–529.

De Schepper, S., Head, M.J., 2008a. Age calibration of dinoflagellate cyst and acritarch events in the Pliocene–Pleistocene of the eastern North Atlantic (DSDP Hole 610A). Stratigraphy 5, 137–161.

De Schepper, S., Head, M.J., 2008b. New dinoflagellate cyst and acritarch taxa from the Pliocene and Pleistocene of the eastern North Atlantic (DSDP Site 610). J. Syst. Palaeont. 6, 101–117.

De Schepper, S., Head, M.J., 2009. Pliocene and Pleistocene dinoflagellate cyst and acritarch zonation of DSDP Hole 610A, eastern North Atlantic. Palynology 33, 179–218.

De Schepper, S., Head, M.J., 2014. New late Cenozoic acritarchs: evolution, palaeoecology and correlation potential in high latitude oceans. J. Syst. Paleont. 12, 493–519.

De Schepper, S., Head, M.J., Louwye, S., 2004. New dinoflagellate cyst and incertae sedis taxa from the Pliocene of northern Belgium, southern North Sea Basin. J. Paleontol. 78, 625–644.

De Schepper, S., Head, M.J., Louwye, S., 2009. Pliocene dinoflagellate cyst stratigraphy, palaeoecology and sequence stratigraphy of the Tunnel-Canal Dock, Belgium. Geol. Mag. 146, 92–112.

De Schepper, S., Fischer, E., Groeneveld, J., Head, M.J., Matthiessen, J., 2011. Deciphering the palaeoecology of Late Pliocene and Early Pleistocene dinoflagellate cysts. Palaeogeogr. Palaeoclimatol. Palaeoecol. 309, 17–32.

De Schepper, S., Groeneveld, J., Naafs, B.D.A., Van Renterghem, C., Hennissen, J., Head, M.J., Louwye, S., Fabian, K., 2013. Northern Hemisphere glaciation during the globally warm early late Pliocene. PLoS ONE 12, e81508. doi:10.1371/journal.pone.0081508

De Schepper, S., Schreck, M., Beck, K.M., Matthiessen, J., Fahl, K., Mangerud, G., 2015. Early Pliocene onset of modern Nordic Seas circulation related to ocean gateway changes. Nat. Commun. 6(8659), doi:10.1038/ncomms9659.

de Vernal, A., Mudie, P., 1989. Pliocene and Pleistocene palynostratigraphy at ODP Sites 646 and 647, eastern and southern Labrador Sea. Proc. ODP Sci. Res. 105, 401–422.

de Verteuil, L., Norris, G., 1996. Miocene dinoflagellate stratigraphy and systematics of Maryland and Virginia. Micropaleontology 42, 1–172.

Donnally, D.M., 1989. Calcareous nannofossils of the Norwegian-Greenland Sea: ODP leg 104. Proc. ODP Sci. Res. 104, 459–486.

Dybkjær, K., Piasecki, S., 2010. Neogene dinocyst zonation for the eastern North Sea Basin, Denmark. Rev. Palaeobot. Palynol. 161, 1–29.

Fensome, R.A., MacRae, R.A., Williams, G.L., 2008. DINOFLAJ2, version 1. AASP Data Series 1. URL http://dinoflaj.smu.ca/Wiki/Main_Page.

Goll, R.M., Bjørklund, K.R., 1989. A New Radiolarian Biostratigraphy for the Neogene of the Norwegian Sea: ODP Leg 104. Proc. ODP Sci. Res. 104, 697–737.

Grøsfjeld, K., De Schepper, S., Fabian, K., Husum, K., Baranwal, S., Andreassen, K., Knies, J., 2014. Dating and palaeoenvironmental reconstruction of the sediments around the Miocene/Pliocene boundary in Yermak Plateau ODP Hole 911A using marine palynology. Palaeogeogr. Palaeoclimatol. Palaeoecol. 414, 382–402.

Head, M.J., 1993. Dinoflagellates, sporomorphs and other palynomorphs from the Upper Pliocene St. Erth Beds of Cornwall, southwestern England. J. Paleontol. Memoir 31, 1–62.

Head, M.J., 1996. Late Cenozoic dinoflagellates from the Royal Society Borehole at Ludham, Norfolk, Eastern England. J. Paleontol. 70, 543–570.

Head, M.J., 1997. Thermophilic dinoflagellate assemblages from the mid Pliocene of eastern England. J. Paleontol. 71, 165–193.

Head, M.J., 1998. Marine environmental change in the Pliocene and early Pleistocene of eastern England; the dinoflagellate evidence reviewed. In: van Kolfschoten, T., Gibbard, P.L. (Eds.), The Dawn of the Quaternary, Mededelingen Nederlands Instituut voor Toegepaste Geowetenschappen TNO 60, pp. 199–226.

Head, M.J., Norris, G., 2003. New species of dinoflagellate cysts and other palynomorphs from the latest Miocene and Pliocene of DSDP hole 603C, western North Atlantic. J. Paleontol. 77, 1–15.

Head, M.J., Westphal, H., 1999. Palynology and paleoenvironments of a Pliocene carbonate platform: The Clino core, Bahamas. J. Paleontol. 73, 1–25.

Hilgen, F.J., Lourens, L.J., Van Dam, J.A., Beu, A.G., Boyes, A.F., Cooper, R.A., Krijgsman, W., Ogg, J.G., Piller, W.E., Wilson, D.S., 2012. The Neogene Period. In: Gradstein, F., Ogg, J.G., Schmitz, M., Ogg, G. (Eds.), The Geologic Time Scale 2012. Elsevier, Amsterdam, The Netherlands, pp. 923–978.

Jansen, E., Fronval, T., Rack, F., Channell, J., 2000. Pliocene-Pleistocene ice rafting history and cyclicity in the Nordic Seas during the last 3.5 Myr. Paleoceanography 15, 709–721.

Knies, J., Cabedo-Sanz, P., Belt, S.T., Baranwal, S., Fietz, S., Rosell-Melé, A., 2014. The emergence of modern sea ice cover in the Arctic Ocean. Nat. Commun. 5(5608), doi:10.1038/ncomms6608.

Limoges, A., Londeix, L., de Vernal, A., 2013. Organic-walled dinoflagellate cyst distribution in the Gulf of Mexico. Mar. Micropaleontol. 102, 51–68. doi:10.1016/j.marmicro.2013.06.002

Lourens, L.J., Hilgen, F.J., Laskar, J., Shackleton, N.J., Wilson, D., 2005. The Neogene. In: Gradstein, F., Ogg, J.G., Smith, A. (Eds.), A Geological Time Scale 2004, Cambridge University Press, Cambridge, UK, pp. 409–430.

Louwye, S., 1999. New species of organic-walled dinoflagellates and acritarchs from the Upper Miocene Diest Formation, northern Belgium (southern North Sea Basin). Rev. Palaebot. Palynol. 107, 109–123.

Louwye, S., De Schepper, S., 2010. The Miocene–Pliocene hiatus in the southern North Sea Basin (northern Belgium) revealed by dinoflagellate cysts. Geol. Mag. 147, 760–776.

Louwye, S., Head, M.J., De Schepper, S., 2004. Dinoflagellate cyst stratigraphy and palaeoecology of the Pliocene in northern Belgium, southern North Sea Basin. Geol. Mag. 141, 353–378.

Manum, S.B., Boulter, M.C., Gunnarsdottir, H., Rangnes, K., Scholze, A., 1989. Eocene to Miocene palynology of the Norwegian Sea (ODP Leg 104). Proc. ODP Sci. Res. 104, 611–662.

Matthiessen, J., Brinkhuis, H., Poulsen, N.E., Smelror, M., 2009a. *Decahedrella martinheadii* Manum 1997 – a stratigraphically and paleoenvironmentally useful Miocene acritarch of the high northern latitudes. Micropaleontology 55, 171–186.

Matthiessen, J., Knies, J., Vogt, C., Stein, R., 2009b. Pliocene palaeoceanography of

the Arctic Ocean and subarctic seas. Phil. Trans. A Math. Phys. Eng. Sci. 367, 21–48.

Mattingsdal, R., Knies, J., Andreassen, K., Fabian, K., Husum, K., Grøsfjeld, K., De Schepper, S., 2013. A new 6 Myr stratigraphic framework for the Atlantic–Arctic Gateway. Quat. Sci. Rev. 92, 170–178.

Moran, K., Backman, J., Brinkhuis, H., Clemens, S.C., Cronin, T., Dickens, G.R., Eynaud, F., Gattacceca, J., Jakobsson, M., Jordan, R.W., Kaminski, M., King, J., Koç, N., Krylov, A., Martinez, N., Matthiessen, J., McInroy, D., Moore, T.C., Onodera, J., O'Regan, M., Pälike, H., Rea, B., Rio, D., Sakamoto, T., Smith, D.C., Stein, R., St John, K., Suto, I., Suzuki, N., Takahashi, K., Watanabe, M., Yamamoto, M., Farrell, J., Frank, M., Kubik, P., Jokat, W., Kristoffersen, Y., 2006. The Cenozoic palaeoenvironment of the Arctic Ocean. Nature 441, 601–605.

Mudie, P., 1989. Palynology and dinocyst biostratigraphy of the late Miocene to Pleistocene, Norwegian Sea; ODP Leg 104, Sites 642 and 644. Proc. ODP Sci. Res. 104, 587–610.

Munsterman, D.K., Brinkhuis, H., 2004. A southern North Sea Miocene dinoflagellate cyst zonation. Neth. J. Geosci. 83, 267–285.

Murphy, M.A., Salvador, A., 1999. International Stratigraphic Guide — An abridged version. Episodes 22, 255–271.

Paez-Reyes, M., Head, M.J., 2013. The Cenozoic gonyaulacacean dinoflagellate genera *Operculodinium* Wall, 1967 and *Protoceratium* Bergh, 1881 and their phylogenetic relationships. J. Paleontol. 87, 786–803.

Piasecki, S., 1980. Dinoflagellate cyst stratigraphy of the Miocene Hodde and Gram Formations, Denmark. Bull. Geol. Soc. Denmark 29, 53–76.

Piasecki, S., 2003. Neogene dinoflagellate cysts from Davis Strait, offshore West Greenland. Mar. Petr. Geol. 20, 1075–1088.

Risebrobakken, B., Andersson, C., De Schepper, S., McClymont, E.L., submitted. High-amplitude, low frequency Pliocene climate variability – identifying climate phases and transitions in the eastern Nordic Seas. Paleoceanography, 1–44.

Schreck, M., Matthiessen, J., 2013. *Batiacasphaera micropapillata*: Palaeobiogeographic distribution and palaeoecological implications of a critical Neogene species complex. In: Lewis, J.M., Marret, F., Bradley, L. (Eds.),

995 Biological and Geological Perspectives of Dinoflagellates. The
996 Micropalaeontological Society, Special Publications. Geological Society
997 London, UK, pp. 293–306.
998Schreck, M., Matthiessen, J., Head, M.J., 2012. A magnetostratigraphic calibration
999 of Middle Miocene through Pliocene dinoflagellate cyst and acritarch events
1000 in the Iceland Sea (Ocean Drilling Program Hole 907A). Rev. Palaebot.
1001 Palynol. 187, 66–94.
1002Shipboard Scientific Party, 1987. Site 642: Norwegian Sea. Proc. ODP Init. Rep.
1003 104, 53–453.
1004Spiegler, D., Jansen, E., 1989. Planktonic foraminifer biostratigraphy of Norwegian
1005 Sea sediments: ODP Leg 104. Proc. ODP Sci. Res. 104, 681–696.
1006Stein, R., Fahl, K., Schreck, M., Knorr, G., Niessen, F., Forwick, M., Gebhardt, C.,
1007 Jensen, L., Kaminski, M., Kopf, A., Matthiessen, J., Jokat, W., Lohmann, G., 2016.
1008 Evidence for ice-free summers in the late Miocene central Arctic Ocean. Nat.
1009 Commun. 7, 11148, doi: 10.1038/ncomms11148.
1010Verhoeven, K., Louwye, S., Eiríksson, J., De Schepper, S., 2011. A new age model
1011 for the Pliocene-Pleistocene Tjörnes section on Iceland: Its implication for
1012 the timing of North Atlantic-Pacific palaeoceanographic pathways.
1013 Palaeogeogr. Palaeoclimatol. Palaeoecol. 309, 33–52.
1014Verhoeven, K., Louwye, S., Paez-Reyes, M., Mertens, K.N., Vercauteren, D., 2014.
1015 New acritarchs from the late Cenozoic of the southern North Sea Basin and
1016 the North Atlantic realm. Palynology 38, 38–50.
1017Versteegh, G., Zevenboom, D., 1995. New genera and species of dinoflagellate
1018 cysts from the Mediterranean Neogene. Rev. Palaebot. Palynol. 85, 213–229.
1019Wall, D., Dale, B., 1966. “Living fossils” in Western Atlantic plankton. Nature 211,
1020 1025–1026.
1021

FIGURE CAPTIONS

Figure 1. Bathymetric map of the Nordic Seas showing the location of ODP Site 642 in the Norwegian Sea and the other locations in the Iceland Sea (ODP Site 907), the North Atlantic (DSDP Site 610) and the North Sea Basin discussed in the text.

Figure 2. ODP Hole 642B lithology, studied samples (core, section and depth (cm) in section are indicated) and stratigraphic occurrence of selected dinoflagellate cysts and acritarch taxa and biozones defined in this study. Grey shading in the biozonation indicate the intervals between the biozones that were not sampled. All raw data are available from the range charts in the appendix and from http://doi.pangaea.de/10.1594/PANGAEA.846838.

Figure 3. Comparison of the new zonation at ODP Hole 642B to the palaeomagnestratigraphy (Bleil, 1989) and previously established zonations using dinoflagellate cysts (Mudie, 1989), planktonic foraminifers (Spiegler and Jansen, 1989), radiolarians (Goll and Bjørklund, 1989), and calcareous nannofossils (Donnally, 1989). Grey shading indicates intervals between the biozones that were not sampled, i.e. the interval between the sample with the highest occurrence of a taxon and the next sample above.

Figure 4. Early and Late Pliocene stratigraphic ranges of selected dinoflagellate cysts in the Norwegian Sea ODP Hole 642B (this study), Iceland Sea ODP Hole 907A (Schreck et al., 2012), eastern North Atlantic DSDP Hole 610A (De Schepper and Head, 2009; 2008a), western North Atlantic DSDP Hole 603C (M.J.

Head, unpublished data) and Labrador Sea ODP Hole 646B (de Vernal and Mudie, 1989). The biozonation of the Norwegian Sea (this study) is compared to zonations in Denmark (Dybkjær and Piasecki, 2010) and the eastern North Atlantic (De Schepper and Head, 2009). Correlations of the zonal boundaries using the marker species between the different zonations is shown. Correlation of individual taxa with the Danish zonation is approximate and does not reflect precise absolute ages derived from within the Danish North Sea basin. Abbreviations used: Oteg = *O. tegillatum*, Bmin = *B. minuta*/*B. micropapillata* complex, Cdev = *C. devernaliae*, Bgr = *B. graminosum*, Ilac = *I. lacrymosa*, Mcho = *M. choanophorum*, Isol = *I. solidum*.

TABLE CAPTIONS

Table 1. Samples studied from ODP Hole 642B, dry weight of sediment processed for palynology, counts of *Lycopodium clavatum* spike added, and counts and concentrations of dinoflagellate cyst, acritarchs and terrestrial palynomorphs.

Table 2. Magnetostratigraphic reversals in ODP Hole 642B identified by Bleil (1989) and updated to Geological Time Scale 2012 (Hilgen et al. 2012).

Table 3. Highest (HO) and lowest (LO) occurrence of dinoflagellate cysts and acritarchs (indicated by asterisk) in ODP Hole 642B, including estimated age and error (based on sampling interval).

APPENDIX

The appendix contains stratigraphic range charts containing the raw data (counts) of dinoflagellate cysts and acritarchs for ODP Hole 642B. Red shading shows taxa used for defining the biozones, green shading shows taxa with important stratigraphic ranges.

PLATE CAPTIONS

Plate I

Sample code follows ODP nomenclature, listing Site, Hole, Core, Section and depth (cm) in section. England Finder references and slide number are also given. All photographs are taken in transmitted light. 1,2. *Achomosphaera andalousiensis andalousienis* Jan du Chene, 1977 emend. Jan du Chene and Londeix, 1988. ODP 642B-11H-3, 65–66 cm, W45/0, slide 11J501. Uncertain view at (1) high focus on characteristic fenestrate process tip, and at (2) mid-focus showing the free archeopyle. 3,4. *Ataxiodinium confusum* Versteegh and Zevenboom in Versteegh, 1995. ODP 642B-9H-2, 65–66 cm, B55/2, slide 12F475. Oblique dorsal view at (3) high focus on archeopyle and granular wall, and at (4) mid-focus demonstrating the dorsal and ventral connections between endo- and periphragm. 5,6. *Ataxiodinium choane* Reid, 1974. ODP 642B-10H-1, 40–41 cm, Y67/1, slide 12G102. Ventral view at (1) mid-focus with view on faintly granular pericyst, and at (2) low focus on archeopyle. 7,8. *Ataxiodinium zevenboomii* Head, 1997. ODP 642B-11H-7, 15–16 cm, V64/0, slide 11J512. Dorsal/apical? view at (7) high focus on archeopyle and dorsal/apical surface, and (8) mid-focus. 9,10. *Amiculosphaera umbraculum* Harland, 1979. ODP 642B-9H-1, 120–121 cm, Y38/2, slide 12F407. Dorsal view at (9) mid-focus on antapical funnel-shaped connection between peri- and endophragm, and at (10) low focus revealing traces of tabulation (cingulum?) on the periphragm. Note the apical boss on the endophragm (9). 11,12. *Cerebrocysta poulsenii* de Verteuil and Norris, 1996. ODP 642B-11H-7, 55–56 cm, T31/2, slide 11J513. Oblique dorsal view at (11) high focus on granulate wall and at (12) mid-focus. 13. *Barssidinium pliocenicum* (Head, 1993) De Schepper and Head, 2004. ODP 642B-9H-3, 70–71 cm, G51/1,

slide 12G12. Vertical stack of several foci. 14,15. *Dapsilidinium pastielsii* (Davey and Williams, 1966) Bujak, Downie, Eaton and Williams, 1980. ODP 642B-9H-2, 65–66 cm, J48/3, slide 12F475. Antapical view of (14) high focus on granulate wall, and at (15) mid-focus. 16. *Heteraulacacysta* sp. A of Costa and Downie, 1979. ODP 642B-9H-3, 70–71 cm, G33/2, slide 12G12. Vertical stack of several foci. 17, 18. *Impagidinium aculeatum* (Wall, 1967) Lentin and Williams, 1981. ODP 642B-9H-3, 60–61 cm, J41/1, slide 12G10. Dorsal view at (17) high focus on archeopyle (3''), and at (18) mid-focus. 19, 20. *Impagidinium pallidum* Bujak, 1984. ODP 642B-9H-3, 70–71 cm, E32/3, slide 12G12. Dorsal view at (19) high focus on archeopyle (3''), illustrating the incomplete expression of the tabulation, and at (20) mid-focus.

Plate II

Sample code follows ODP nomenclature, listing Site, Hole, Core, Section and depth (cm) in section. England Finder references and slide number are also given. All photographs are taken in transmitted light. 1–3. *Batiacasphaera hirsuta* Stover, 1977. ODP642B-11H-3, 65–66 cm, W54/0, slide 11J501. Uncertain view at slightly different high foci (1,2) illustrating the pili (hairs) characteristic for this species and the apical archeopyle at the top, and at (3) mid-focus. 4, 8. *Invertocysta lacrymosa* Edwards, 1984. ODP 642B-9H-3, 60–61 cm, O50/1, slide 12G10. Dorsal view at (4) high focus, and at (8) low focus showing an apical boss on the endocyst. 5–7. *Batiacasphaera micropapillata* complex sensu Schreck and Matthiessen, 2013. ODP 642B, 11H3, 65–66 cm, M43/3, slide 11J501. Apical view at (5) high focus on apical archeopyle and microreticulate wall ornament, at (6) mid-focus, and at (7) low focus on antapical surface. 9–16. *Bitectatodinium* sp. A.

(9–12) ODP 642B-8H-6, 129–130 cm, F34/0, slide 12F401. Ventral view at slightly different high foci (9,10) illustrating a dense ornament of pili and short ridges ("columellate") on the wall revealed by L(ux)–O(bscura) analysis; at (11) mid-focus and at (12) low focus on 2P archeopyle. (13–16) ODP 642B-8H-6, 129–130 cm, G35/0, slide 12F401. Dorsal view at (13,14) high focus on 2P archeopyle and dense wall ornament of pili and short ridges ("columellate"); at (15) mid-focus and at (16) low focus on ventral surface. 17–20. *Melitasphaeridium choanophorum* (Deflandre and Cookson 1955) Harland and Hill, 1979. ODP 642B-9H-2, 65–66 cm, K48/3, slide 12F475. Oblique ventral view at (17) high focus on aculeate process tips; at (18) slightly lower high focus on granular wall; at (19) mid-focus ad at (20) lower focus on 3'' archeopyle.

Plate III

Sample code follows ODP nomenclature, listing Site, Hole, Core, Section and depth (cm) in section. England Finder references and slide number are also given. All photographs are taken in transmitted light. 1–3. *Corrudinium*? *labradori* Head, Norris and Mudie, 1989. ODP 642B-10H-4, 15–16 cm, X56/0, slide 11J378

Dorsal view at (1) high focus on 2P archeopyle, reticulate wall ornament and cingulum expressed by single margin; at (2) mid-focus and at (3) ventral surface with expressed cingulum and possibly one margin of the sulcal area. 4,8. *Filisphaera filifera* subsp. *filifera* Bujak, 1984 emend. Head, 1994. ODP642-9H-2, 65–66 cm, B53/4, slide 12F475. Oblique view at (4) high focus on finely reticulate wall with smaller and larger lumina, and at (8) mid-focus illustrating the radiating septa of the luxuria. 5–7. *Corrudinium devernaliae* Head and Norris,

2003. ODP 642B-10H-1, 145–146 cm, L55/0, slide 12G104. Oblique dorsal view at (5) high focus on archeopyle and crests that form an incomplete and large reticulum; at (6) mid-focus and at (7) low focus on ventral surface. 9–11. *Habibacysta tectata* Head, Norris and Mudie, 1989. ODP 642B-8H-6, 129–130 cm, N35/1, slide 12F401. Ventral view at (9) high focus showing the characteristic wall ornament, at (10) mid-focus, and at (11) lower focus on the 3'' archeopyle and dorsal surface. 12,16. "*Impagidinium densiverrucosum*" of Zevenboom and Santarelli in Zevenboom (1995). ODP 642B-11H-7, 55–56 cm, U37/2, slide 111J513. Dorsal view at (12) high focus on precingular archeopyle (free) and coarsely verrucate wall ornament, and at (16) mid-focus. Note the 3'' precingular operculum central in the picture. 13,14. *Pyxidinopsis braboi* De Schepper and Head, 2004. ODP 642B-9H-1, 120–121 cm, D52/2, slide 12F407 Oblique dorsal view at (13) high focus and at (14) mid-focus. 15. *Selenopemphix nephroides* Benedek, 1972 emend. Bujak in Bujak, Downie, Eaton and Williams, 1980. ODP 642B-9H-3, 60–61 cm, W39/3, slide 12G10. Vertical stack of several foci. 17,18. *Operculodinium janduchenei* Head, Norris and Mudie, 1989. ODP 642B-9H-2, 65–66 cm, J46/2, slide 12F475. Dorsal view at (17) high focus and at (18) mid-focus. Processes on this specimen are somewhat long compared to originally illustrated specimens in Head, Norris and Mudie, 1989. 19,20. Cyst of *Pentapharsodinium dalei* Indelicato and Loeblich III 1986. ODP 642B-9H-6, 100–101 cm, M61/0, slide 12G98. Uncertain view at subsequently lower foci (19,20) showing the solid processes that occasionally branch.

Plate IV

Sample code follows ODP nomenclature, listing Site, Hole, Core, Section and depth (cm) in section. England Finder references and slide number are also given. All photographs are taken in transmitted light. 1–3, 5–7. *Operculodinium*? *eirikianum* var. *eirikianum* Head, Norris and Mudie, 1989 emend. Head, 1997. (1–3) ODP 642B-9H-3, 55–56 cm, V39/0, slide 12G9. Dorsal view at (1) high focus on large precingular archeopyle (3''), at (2) mid-focus, and at (3) lower focus. (5–7) ODP 642B-11H-5, 60–61 cm, X38/2, slide 11J507. Ventral view at (5) high focus on ventral surface, at (6) mid-focus, and at (7) low focus on dorsal surface with archeopyle. 4,8. *Operculodinium*? *eirikianum* var. *crebrum* De Schepper and Head, 2008. ODP 642B-9H-3, 60–61 cm, O49/0, slide 12G10. Uncertain view at (4) high focus on microreticulate wall structure and at (8) mid-focus. Note the very thick luxuria [2.5–3.0 μm], consisting of radiating, non-tabular septa. 9–11, 12,16. *Operculodinium tegillatum* Head, 1997. (9–11) ODP 642B-10H-1, 145–146 cm, L56/0, slide 12G104. Apical view at (9) high focus showing the precingular archeopyle (3''), at (10) mid-focus, and at (11) lower focus. (12,16). ODP 642B-10H-3, 102–103 cm, S62/0, slide 12G135. Uncertain view at (12) high focus and at (16) mid-focus. 13,14. *Spiniferites elongatus* Reid, 1974. ODP 642B-9H-2, 65–66 cm, D57/2, slide 12F475. Dorsal view at (13) high focus and at (14) mid-focus. 15. *Selenopemphix brevispinosa* Head, Norris and Mudie, 1989. ODP 642B-11H-7, 15–16 cm, V35/0, slide 11J512. Vertical stack of several foci. 17–20. *Reticulatosphaera actinocoronata* (Benedek, 1972) Bujak and Matsuoka, 1986. (17–18) ODP 642B-10H-2, 40–41 cm, C48/0, slide 12G105. Uncertain view at (17) high focus on the irregularly branching process tips and at (18) mid-focus. (19–20) ODP 642B-10H-3, 102–103 cm, M37/0, slide 12G135. Uncertain view at

(19) high focus and at (20) mid-focus. Arrow indicates possible opercular plate with a single process.

Plate V

Sample code follows ODP nomenclature, listing Site, Hole, Core, Section and depth (cm) in section. England Finder references and slide number are also given. All photographs are taken in transmitted light. 1–7. Cyst type I of de Vernal and Mudie (1989). (1–4) ODP 642B-10H-2, 40–41 cm, L40/3, slide 12G105. Uncertain view at (1) high focus on granular trabeculae forming a network with circular openings, at two slightly different mid-foci (2,3) showing numerous, thin solid processes ending distally in broad, ornamented trabeculae, and at (4) low focus on (apical?) archeopyle. (5–7) ODP 642B-10H-2, 40–41 cm, N41/0, slide 12G105. Uncertain view at (1) high focus, at (6) mid-focus, and at (7) low focus on (apical?) archeopyle. 8,12–16. *Lavradosphaera canalis*. (8,12) ODP 642B-11H-6, 70–71 cm, W42/1, slide 11J510. Uncertain view at (8) high focus and (12) low focus. (13–16) ODP 642B-11H-6, 70–71 cm, W49/3, slide 11J510. Antapical view at (13) high focus, at two slightly different mid-foci (14,15) showing the U-shaped channels typical of *Lavradosphaera canalis*, and at (16) low focus on pylome. 9–11. "*Veriplicidium franklinii*" of Anstey (1992). ODP 642B-11H-7, 15–16 cm, W32/0, slide 11J512. Uncertain view at (9) high focus, (8) mid-focus and (11) lower focus. 17–20. *Lavradosphaera*? sp.. ODP 642B-10H-3, 102–103 cm, O56/3, slide 12G135. Two slightly different high foci (17,18), mid-focus (19) and low focus (20) revealing outline of pylome.

Plate VI

Sample code follows ODP nomenclature, listing Site, Hole, Core, Section and depth (cm) in section. England Finder references and slide number are also given. All photographs are taken in transmitted light. 1–3. *Gelasinicysta vangeelii* Head, 1992. ODP 642B-10H-4, 15–16 cm, X57/3, slide 11J378. High focus (1), mid-focus (2) and low focus (3). 4. *Pediastrum.* ODP 642B-9H-3, 60–61 cm, C45/2, slide 12G10. 5–7. *Cymatiosphaera*? *aegirii* De Schepper and Head, 2014. ODP 642B-9H-3, 70–71 cm, H45/2, slide 12G12. Slightly lower high foci (5,6) on trifurcate process tips that connect to the next process via thin, round and solid trabeculae, and mid-focus (7). 8,12,16. *Cymatiosphaera*? *invaginata* Head, Norris and Mudie, 1989. (8,12) ODP 642B-9H-3, 70–71 cm, Q49/0, slide 12G12 High focus (8) on undulating crests and mid-focus (12) showing the Y-shaped distal ends of the crests. (16) ODP 642B-9H-3, 60–61 cm, W37/3, slide 12G10. Mid-focus. 9–11. *Cymatiosphaera*? *icenorum* De Schepper and Head, 2014. ODP 642B-9H-3, 60–61 cm, W37/3, slide 12G10. Slightly different high foci (9,10) showing a broad process typical for the species, and mid-focus (11). 13–14. *Lavradosphaera crista* De Schepper and Head, 2008. ODP 642B-9H-3, 70–71 cm, G46/0, slide 12G12. Apical view at (13) high focus on pylome, resembling an apical archeopyle, and at (14) mid-focus. 15. *Nannobarbophora walldalei* Head, 1996. ODP 642B-9H-3, 60–61 cm, D44/0, slide 12G10.

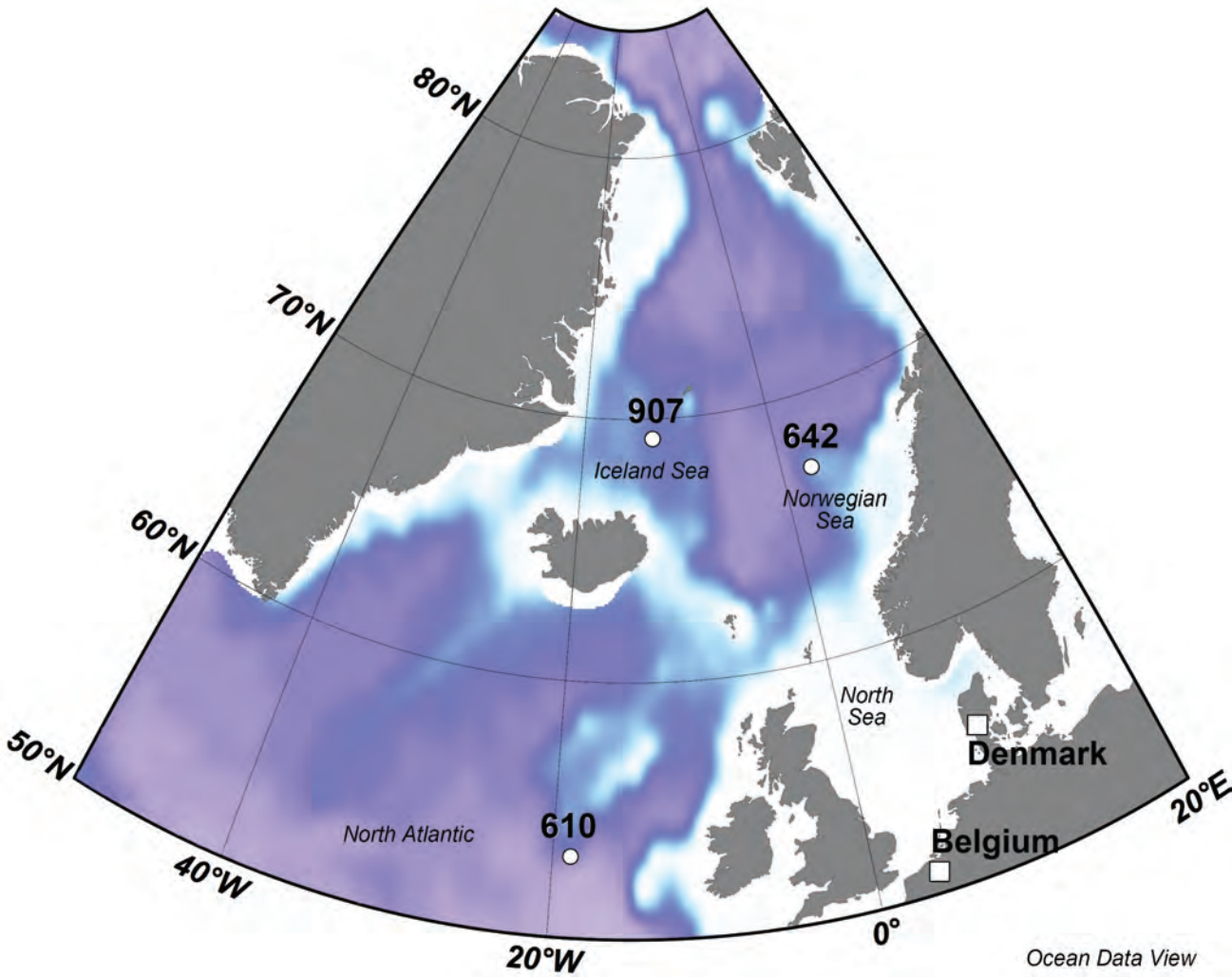
80°N
70°N
60°N
50°N
40°W
20°W
0°
20°E
907
642
610
Iceland Sea
Norwegian Sea
North Sea
North Atlantic
Denmark
Belgium
Ocean Data View

DINOFLAGELLATE CYSTS
ACRITARCHS
Depth (mbsf)
Lithology
Samples
Zonation
A. andalousiensis andalousiensis
A. umbraculum
O.? eirikianum eirikianum
B. pliocenicum
I. pallidum
P. braboi
F. filifera (filifera + pilosa)
Cysts of P. reticulatum
B. raedwaldii
B. graminosum
T. pellitum
B.? serratum
I. lacrymosa
M. choanophorum
A. zevenboomii
C.? labradori
Heteraulacacysta sp. A of Costa & Downie (1979)
O. janduchenei
T. glorianum
A. andalousiensis suttonensis
S. elongatus
A. confusum
O.? eirikianum crebrum
Melitasphaeridium sp. A of De Schepper & Head (2008b)
I. solidum
O. tegillatum
C. devernaliae
Cyst type 1 of de Vernal and Mudie (1989)
R. actinocoronoata
S. brevispinosa
B. micropapillata complex
B. minuta s.s.
C. diminutivum
B. hirsuta
"Impagidinium densiverrucosum" in Zevenboom (1995)
C. poulsenii
S. armageddonensis
Pyxidinopsis sp. A
Cymatiosphaera? invaginata
Lavradosphaera crista
Cymatiosphaera? aegirii
Cymatiosphaera? icenorum
Cymatiosphaera? fensomei
Lavradosphaera lucifer
"Veriplicidium franklinii" in Anstey (1992)
Lavradosphaera canalis
HPO
HCO
UNIT I
UNIT IIA
UNIT IIB
Bioevents
occurrence
occurrence outside regular counts
reworked
acme
Lithology
glacial mud alternates with interglacial sandy mud
nannofossil ooze
siliceous ooze and mud
not zoned
VP3
VP2
VP1

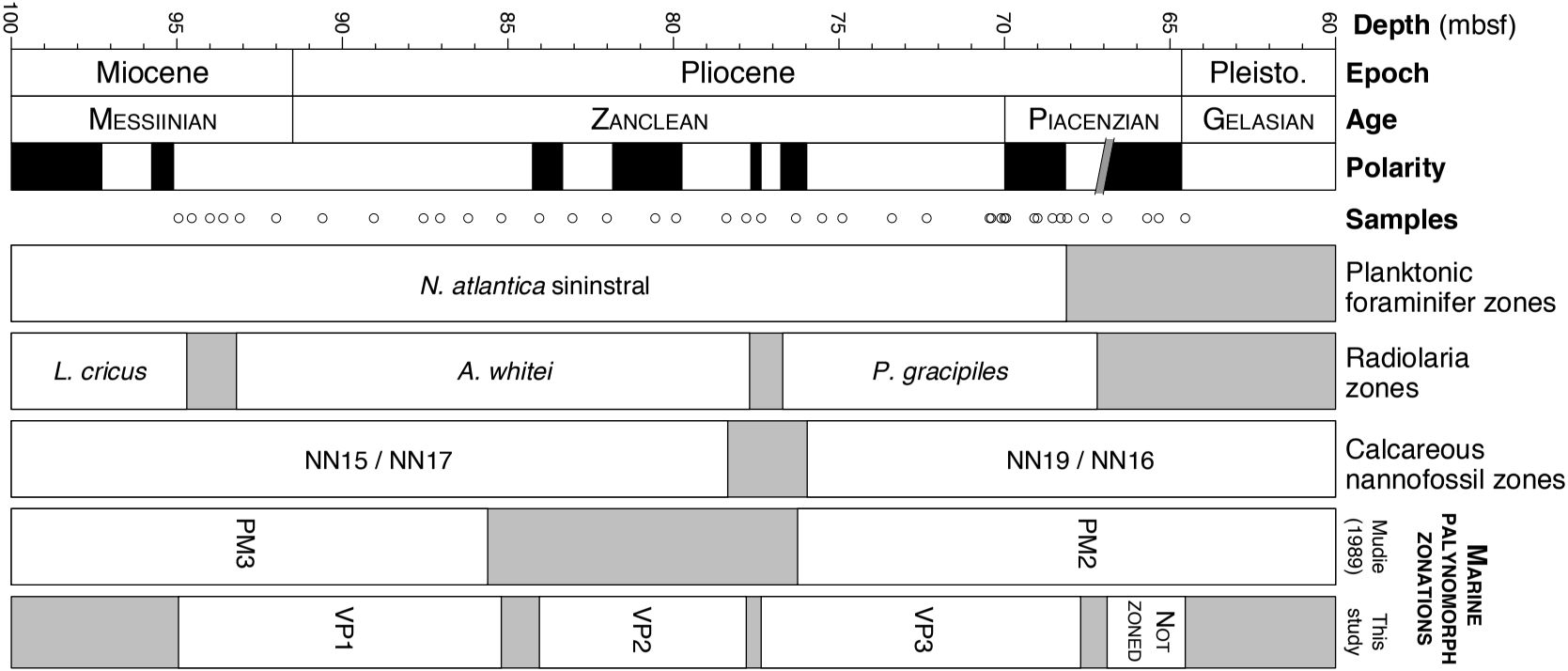
100
95
90
85
80
75
70
65
60
Depth (mbsf)
Miocene
Pliocene
Pleisto.
Epoch
MESSIINIAN
ZANCLEAN
PIACENZIAN
GELASIAN
Age
Polarity
Samples
N. atlantica sininstral
Planktonic foraminifer zones
L. cricus
A. whitei
P. gracipiles
Radiolaria zones
NN15 / NN17
NN19 / NN16
Calcareous nannofossil zones
PM3
PM2
VP1
VP2
VP3
NOT ZONED
Mudie (1989)
This study
MARINE PALYNOMORPH ZONATIONS

LATE PLIOCENE

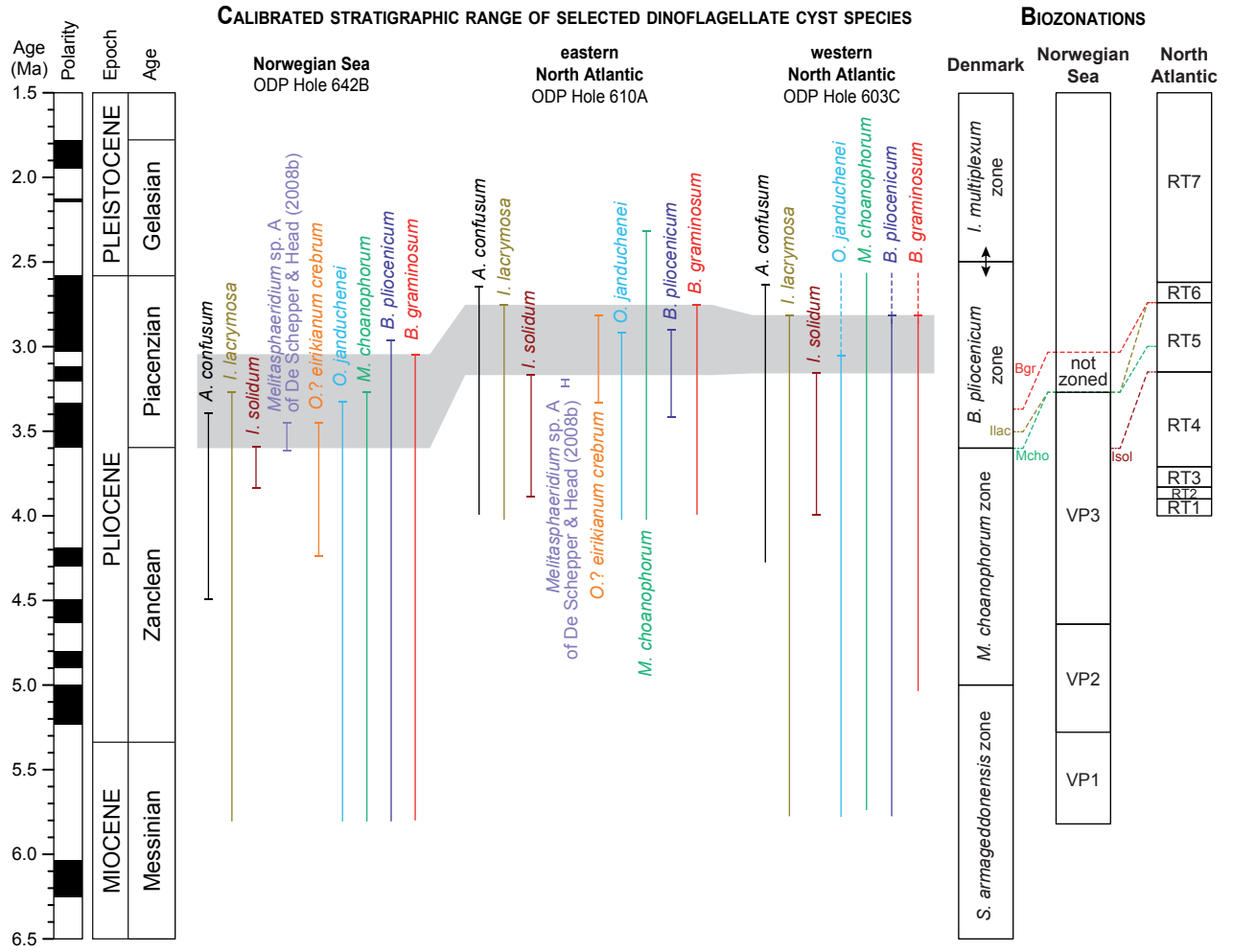

EARLY PLIOCENE

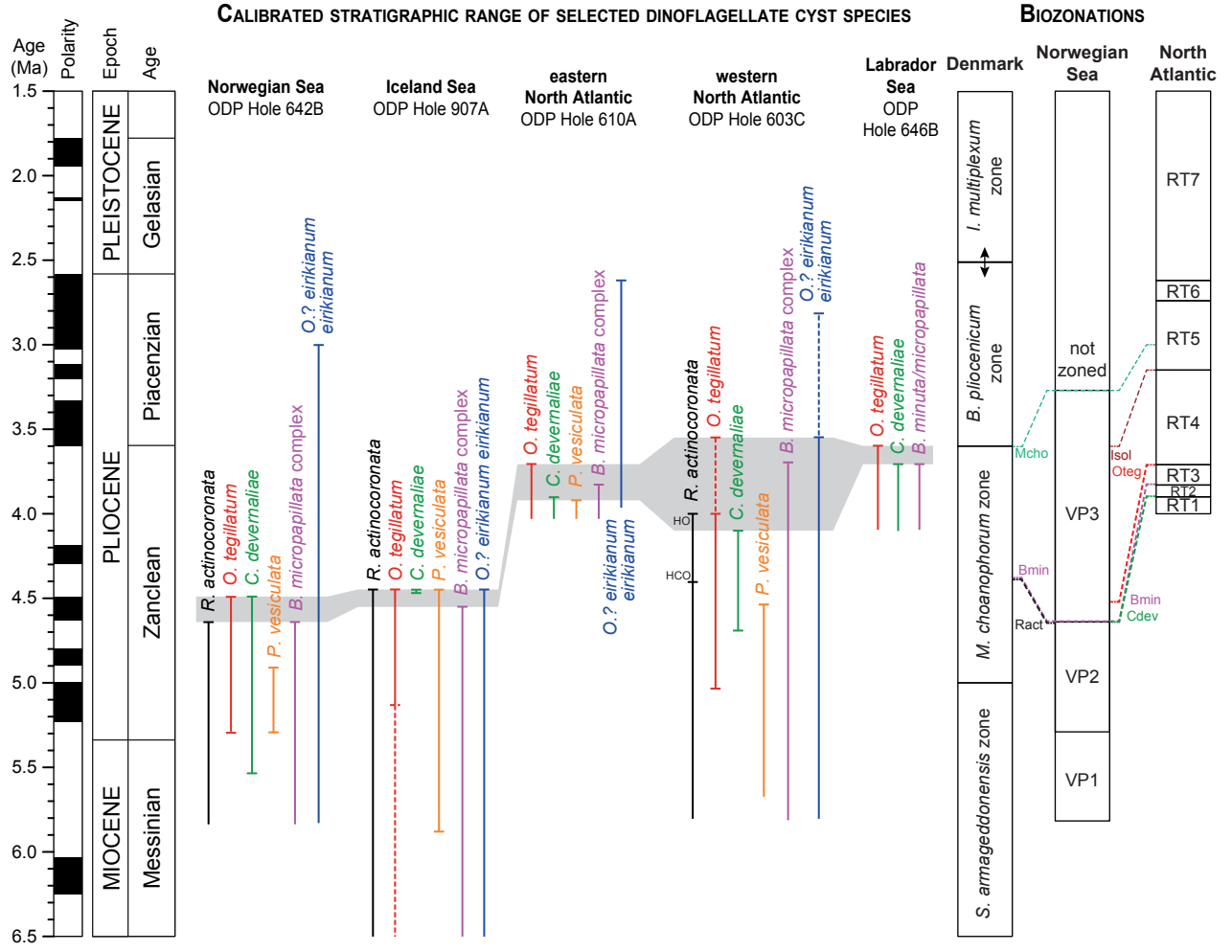

Site	Hole	Core	Section	Interval (cm)	Depth (mbsf)	Calibrated ages (Ma)	Dry weight (g)	*Lycopodium clavatum* tablets added	*Lycopodium clavatum* tablets batch number	No. of *Lycopodium clavatum* grains per tablet	Standard deviation	*Lycopodium clavatum* counted	Dinoflagellate cysts counted (n)	Dinoflagellate cyst concentration (cyst/g)	Dinoflagellate cyst concentration error (cyst/g)	Shannon-Wiener diversity index	Evenness	Reworked dinoflagellate cysts counted (n)	Acritarchs counted (n)	Acritarch concentration (acritarchs/g)	Acritarch concentration error (acritarchs/g)	Terrestrial palynomorphs counted (n)	Terrestrial palynomorphs concentration (grains/g)	Error bar (grains/g)
ODP 642	B	8	6	14–15	64.54	2.96?	9.25	1	483216	18583	1708	248	376	3046	375	2.38	0.71	21	129	1045	149	102	826	123
ODP 642	B	8	6	94–95	65.34	3.04?	14.02	1	483216	18583	1708	824	234	376	44	2.37	0.74	134	90	145	21	624	1004	107
ODP 642	B	8	6	129–130	65.69	3.20–3.04	14.20	1	483216	18583	1708	454	349	1006	117	2.07	0.70	30	94	271	40	177	510	65
ODP 642	B	9	1	50–51	66.90	3.20	6.47	1	483216	18583	1708	182	486	7670	970	1.66	0.57	2	20	316	80	21	331	82
ODP 642	B	9	1	120–121	67.60	3.27	9.53	1	483216	18583	1708	441	332	1468	172	2.34	0.68	9	158	699	91	27	119	26
ODP 642	B	9	2	20–21	68.10	3.32	6.69	1	483216	18583	1708	208	312	4167	535	2.31	0.66		104	1389	210	132	1763	254
ODP 642	B	9	2	40–41	68.30	3.35	10.03	1	483216	18583	1708	169	313	3431	455	2.14	0.56	1	137	1502	221	34	373	78
ODP 642	B	9	2	65–66	68.55	3.39	10.39	1	483216	18583	1708	587	342	1042	119	2.23	0.64	1	42	128	24	52	158	27
ODP 642	B	9	2	110-111	69.00	3.45	13.93	1	483216	18583	1708	101	535	7066	1005	2.23	0.61	+	668	8823	1243	41	542	112
ODP 642	B	9	2	120–121	69.10	3.47	15.31	1	483216	18583	1708	40	390	11834	2246	2.32	0.68	1	312	9467	1813	51	1548	356
ODP 642	B	9	3	55–56	69.95	3.59	10.26	1	483216	18583	1708	110	501	8249	1153	2.12	0.57	+	516	8496	1186	101	1663	275
ODP 642	B	9	3	60–61	70.00	3.60	9.63	1	483216	18583	1708	88	313	6864	1041	2.12	0.55	1	905	19845	2870	76	1667	303
ODP 642	B	9	3	70–71	70.10	3.61	10.17	1	483216	18583	1708	156	320	3748	503	2.51	0.68		659	7719	988	58	679	122
ODP 642	B	9	3	100–101	70.40	3.64	9.87	1	483216	18583	1708	161	435	5087	662	2.05	0.61	1	127	1485	223	20	234	59
ODP 642	B	9	3	105–106	70.45	3.64	8.54	1	483216	18583	1708	233	470	4389	535	2.22	0.65	3	113	1055	155	26	243	55
ODP 642	B	9	4	145–146	72.35	3.83	18.76	1	483216	18583	1708	151	446	2926	385	2.69	0.68	3	1596	10470	1312	176	1155	166
ODP 642	B	9	5	100–101	73.40	3.93	7.40	1	483216	18583	1708	82	425	13015	1974	2.01	0.57	+	1249	38250	5601	112	3430	590
ODP 642	B	9	6	100–101	74.90	4.08	16.32	1	483216	18583	1708	76	279	4180	663	2.34	0.69	2	2432	36437	5407	104	1558	275
ODP 642	B	9	7	11–12	75.51	4.14	5.98	1	483216	18583	1708	220	408	5763	716	2.24	0.65	4	1881	26569	3090	200	2825	379
ODP 642	B	10	1	40–41	76.30	4.23	10.89	1	483216	18583	1708	159	306	3284	441	2.12	0.57	1	1184	12707	1586	80	859	142
ODP 642	B	10	1	145–146	77.35	4.49	6.74	1	483216	18583	1708	52	324	17179	3013	2.38	0.71	2	1	53	54	10	530	189
ODP 642	B	10	2	40–41	77.80	4.64	8.50	1	483216	18583	1708	19	408	46947	11833	2.27	0.63	2	825	94929	23693	95	10931	2925
ODP 642	B	10	2	100–101	78.40	4.69	11.92	1	483216	18583	1708	9	389	67382	23548	2.27	0.60		733	126970	44153	47	8141	3055
ODP 642	B	10	3	102–103	79.92	4.81	11.84	1	483216	18583	1708	25	432	27121	6111	2.53	0.71	1	425	26682	6014	53	3327	863
ODP 642	B	10	4	15–16	80.55	4.84	10.15	1	483216	18583	1708	111	560	9237	1281	2.33	0.65	+	709	11694	1606	66	1089	197
ODP 642	B	10	5	11–12	82.01	4.91	7.83	1	483216	18583	1708	144	324	5340	726	2.11	0.62		1441	23750	3012	140	2307	346
ODP 642	B	10	5	115–116	83.05	4.98	12.52	1	483216	18583	1708	16	452	41930	11341	2.03	0.56	1	262	24305	6646	67	6215	1821
ODP 642	B	10	6	65–66	84.05	5.18	10.20	1	483216	18583	1708	63	334	9659	1596	2.54	0.72	3	320	9254	1533	170	4916	854
ODP 642	B	10	7	30–31	85.20	5.29	11.38	1	483216	18583	1708	140	319	3721	509	2.63	0.77	1	94	1096	178	325	3791	518
ODP 642	B	11	1	80–81	86.20	5.35	11.85	1	483216	18583	1708	102	468	7195	1027	2.53	0.69	15	265	4074	605	140	2152	343
ODP 642	B	11	2	15–16	87.05	5.41	9.75	1	483216	18583	1708	162	463	5447	706	2.48	0.70	7	314	3694	493	174	2047	292
ODP 642	B	11	2	65–66	87.55	5.44	8.87	1	483216	18583	1708	129	500	8120	1095	1.90	0.56	3	186	3021	444	151	2452	370
ODP 642	B	11	3	65–66	89.05	5.53	7.65	1	483216	18583	1708	174	484	6757	862	2.55	0.67	4	378	5277	685	103	1438	222
ODP 642	B	11	4	70–71	90.60	5.62	8.57	1	483216	18583	1708	186	523	6097	765	2.17	0.61	4	192	2238	309	173	2017	282
ODP 642	B	11	5	60–61	92.00	5.71	7.42	1	483216	18583	1708	350	440	3148	367	2.05	0.59	3	261	1868	230	200	1431	183
ODP 642	B	11	6	20–21	93.10	5.78	9.98	1	483216	18583	1708	51	421	15371	2681	2.63	0.71	1	407	14860	2596	131	4783	904
ODP 642	B	11	6	70–71	93.60	5.81	10.07	1	483216	18583	1708	146	444	5612	743	2.17	0.60	2	176	2225	322	136	1719	259
ODP 642	B	11	6	110–111	94.00	5.83	8.66	1	483216	18583	1708	78	382	10509	1624	2.59	0.71	2	311	8556	1339	80	2201	404
ODP 642	B	11	7	15–16	94.55	5.87	6.86	1	483216	18583	1708	94	513	14784	2144	2.44	0.66	+	448	12910	1885	92	2651	459
ODP 642	B	11	7	55–56	94.95	5.89	10.83	1	483216	18583	1708	64	435	11663	1894	2.34	0.63	+	297	7963	1319	59	1582	320

Chron/Subchron (Beil, 1989)	**Chron/Subchron** (GTS 2012)	**Chron boundary name**	**Upper boundary**		**Lower boundary**		**Mid-depth** (mbsf)	**Age** (Ma) in Bleil (1989)	**Age** (Ma) updated to GTS 2012
			Sample	**Depth** (mbsf)	**Sample**	Depth (mbsf)			
C2AN-2/C2AR-2	C2An.2n/ C2An.2r	Top Mammoth	9H-1, 41	66.81	9H-1, 71	67.11	66.96	3.08	3.207
C2AR-2/C2AN-3	C2An.2r / C2An.3n	Base Mammoth	9H-2, 11	68.01	9H-2, 41	68.31	68.16	3.18	3.330
C2AN-3/C2AR-3	C2An.3n/C2Ar	Top Gilbert	9H-3, 47	69.87	9H-3,71	70.11	69.99	3.40	3.596
C2AR-3/C3N-1	C2Ar/C3n.1n	Top Cochiti	9H-7, 56	75.96	10H-1, 9	75.99	75.98	3.88	4.187
C3N-1/C3R-1	C3n.1n/C3n.1r	Base Cochiti	10H-1, 70	76.60	10H-1, 101	76.91	76.76	3.97	4.300
C3R-1/C3N-2	C3n.1r/C3n.2n	Top Nunivak	10H-1, 130	77.20	10H-2, 11	77.51	77.36	4.10	4.493
C3N-2/C3R-2	C3n.2n/C3n.2r	Base Nunivak	10H-2, 11	77.51	10H-2, 41	77.81	77.66	4.24	4.631
C3R-2/C3N-3	C3n.2r/C3n.3n	Top Sidufjall	10H-3, 71	79.61	10H-3, 100	79.90	79.76	4.40	4.799
C3N-3/C3R-3	C3n.3n/C3N.3r	Base Sidufjall	10H-4, 126	81.66	10H-5, 11	82.01	81.84	4.47	4.896
C3R-3/C3N-4	C3N.3r/C3n.4n	Top Thvera	10H-5, 130	83.2	10H-6, 10	83.5	83.35	4.57	4.997
C3N-4/C3R-4(?)	C3n.4n/C3r	Base Thvera	10H-6, 71	84.11	10H-6, 100	84.4	84.255	4.77	5.235
C3R-4 (?)/(C3A) C3AN-1	C3R/C3An.1n	Top Gilbert	12H-2, 71	97.11	12H-2, 101	97.41	97.26	5.35	6.033

Event	**Species**	**Sample**	**Depth** (mbsf)	**Age** (Ma)	**error** (Ma)
HO	*Corrudinium harlandii*	642B-9H1, 120–121 cm	67.60	3.27	0.07
HO	*Corrudinium*? *labradori*	642B-9H1, 120–121 cm	67.60	3.27	0.07
HO	*Heteraulacacysta* sp. A of Costa and Downie (1979)	642B-9H1, 120–121 cm	67.60	3.27	0.07
HO	*Melitasphaeridium choanophorum*	642B-9H1, 120–121 cm	67.60	3.27	0.07
HO	*Operculodinium janduchenei*	642B-9H2, 20–21 cm	68.10	3.32	0.05
HO	*Ataxiodinium confusum*	642B-9H2, 65–66 cm	68.55	3.39	0.04
HO	*Impagidinium solidum*	642B-9H3, 55–56 cm	68.55	3.59	0.12
HO	*Melitasphaeridium* sp. A of Head and De Schepper (2008)	642B-9H2, 110–11 cm	69.00	3.45	0.07
HO	*Operculodinium*? *eirikianum* var. *crebrum*	642B-9H2, 110–11 cm	69.00	3.45	0.07
HO	*Corrudinium devernaliae*	642B-10H1, 145–146 cm	77.35	4.49	0.26
HO	*Operculodinium tegillatum*	642B-10H1, 145–146 cm	77.35	4.49	0.26
HO	*Batiacasphaera micropapillata* complex	642B-10H2, 40–41 cm	77.80	4.64	0.15
HO	Cyst type I of de Vernal and Mudie (1989)	642B-10H2, 40–41 cm	77.80	4.64	0.15
HO	*Reticulatosphaera actinocoronata*	642B-10H2, 40–41 cm	77.80	4.64	0.15
HO	*Selenopemphix brevispinosa*	642B-10H2, 40–41 cm	77.80	4.64	0.15
HO	*Lavradosphaera lucifer**	642B-10H2, 100–101 cm	78.40	4.69	0.05
HO	*Cristadinium diminutivum*	642B-10H5, 11–12 cm	82.01	4.91	0.07
HO	*Batiacasphaera hirsuta*	642B-10H5, 115–116 cm	83.05	4.98	0.07
HO	"*Impagidinium densiverrucosum*" of Zevenboom and Santarelli in Zevenboom (1995)	642B-10H7, 30–31 cm	85.20	5.29	0.11
HO	*Pyxidinopsis vesiculata*	642B-10H7, 30–31 cm	85.20	5.29	0.11
HO	*"Veriplicidium franklinii"* of Anstey (1992)*	642B-10H7, 30–31 cm	85.20	5.29	0.11
HO	*Cerebrocysta poulsenii*	642B-11H1, 80–81 cm	86.20	5.35	0.06
HO	*Selenopemphix armaggedonensis*	642B-11H2, 15–16 cm	87.05	5.41	0.06
HPO	*Trinovantedinium glorianum*	642B-10H7, 30–31 cm	85.20	5.29	0.11
HPO/HCO	*Batiacasphaera hirsuta*	642B-11H3, 65–66 cm	89.05	5.53	0.09
HCO	*Lavradosphaera crista**	642B-9H1, 120–121 cm	67.60	3.27	0.07
LO	*Melitasphaeridium* sp. A of Head and De Schepper (2008)	642B-9H3, 70–71 cm	70.10	3.61	0.03
LO	*Impagidinium solidum*	642B-9H4, 145–146 cm	72.35	3.83	0.10
LO	*Operculodinium*? *eirikianum* var. *crebrum*	642B-10H1, 40–41 cm	76.30	4.23	0.26
LO	*Ataxiodinium confusum*	642B-10H1, 145–146 cm	77.35	4.49	0.15
LO	Cyst type I of de Vernal and Mudie (1989)	642B-10H5, 11–12 cm	82.01	4.91	0.07
LO	*Filisphaera filifera* subsp. *filifera*	642B-10H6, 65–66 cm	84.05	5.18	0.11
LO	*Bitectatodinium tepikiense*	642B-10H6, 65–66 cm	84.05	5.18	0.11
LO	*Heteraulacacysta* sp. A of Costa and Downie (1979)	642B-10H7, 30–31 cm	85.20	5.29	0.06
LO	*Operculodinium tegillatum*	642B-10H7, 30–31 cm	85.20	5.29	0.06
LO	*Pyxidinopsis vesiculata*	642B-10H7, 30–31 cm	85.20	5.29	0.06
LO	*Corrudinium devernaliae*	642B-11H3, 65–66 cm	89.05	5.53	0.10

Norwegian Sea ODP Site 642

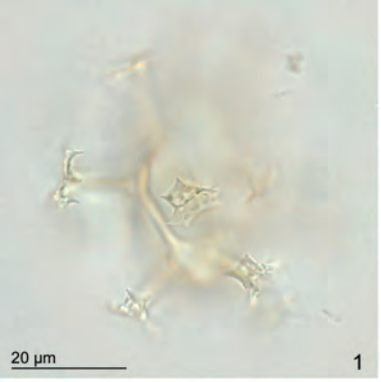
20 µm
1

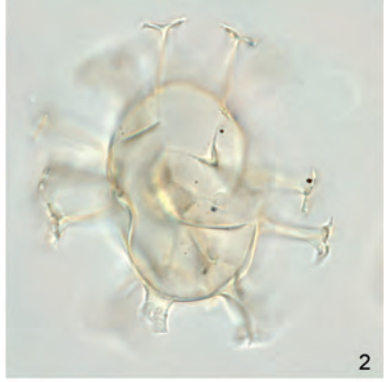
2

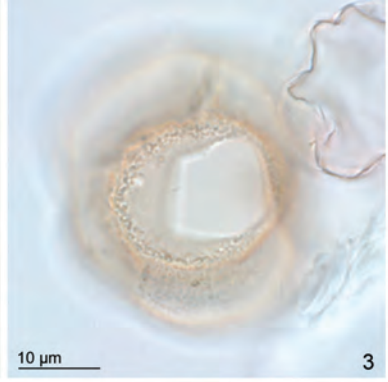
10 µm
3

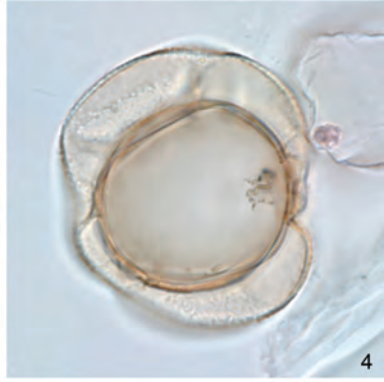
4


20 µm
5


6


20 µm
7

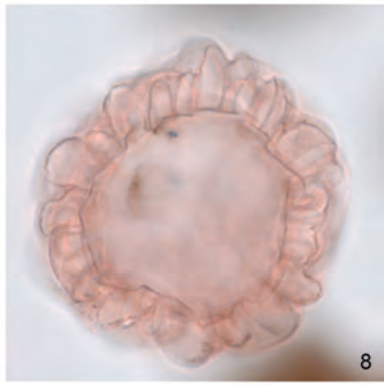
8

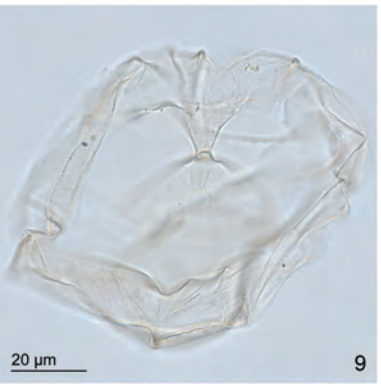
20 µm
9


10

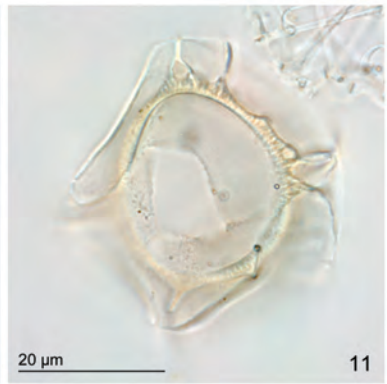
20 µm
11

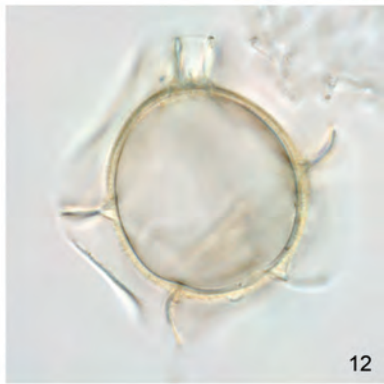
12


20 µm
13

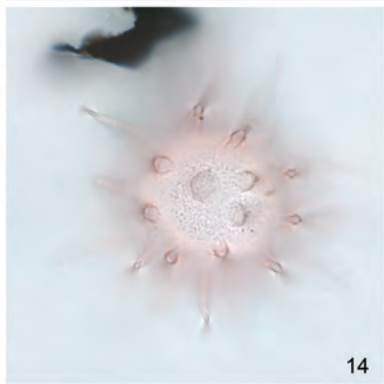
14


20 µm
15

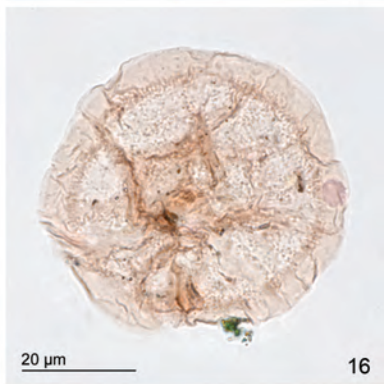
20 µm
16


20 µm
17

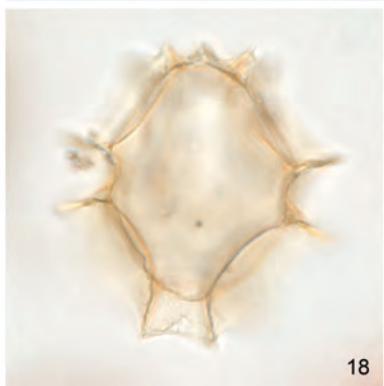
18

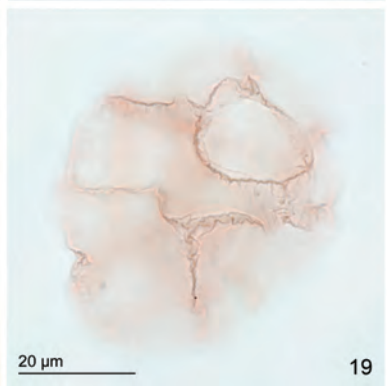
20 µm
19

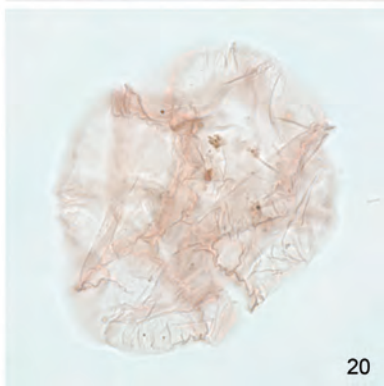
20

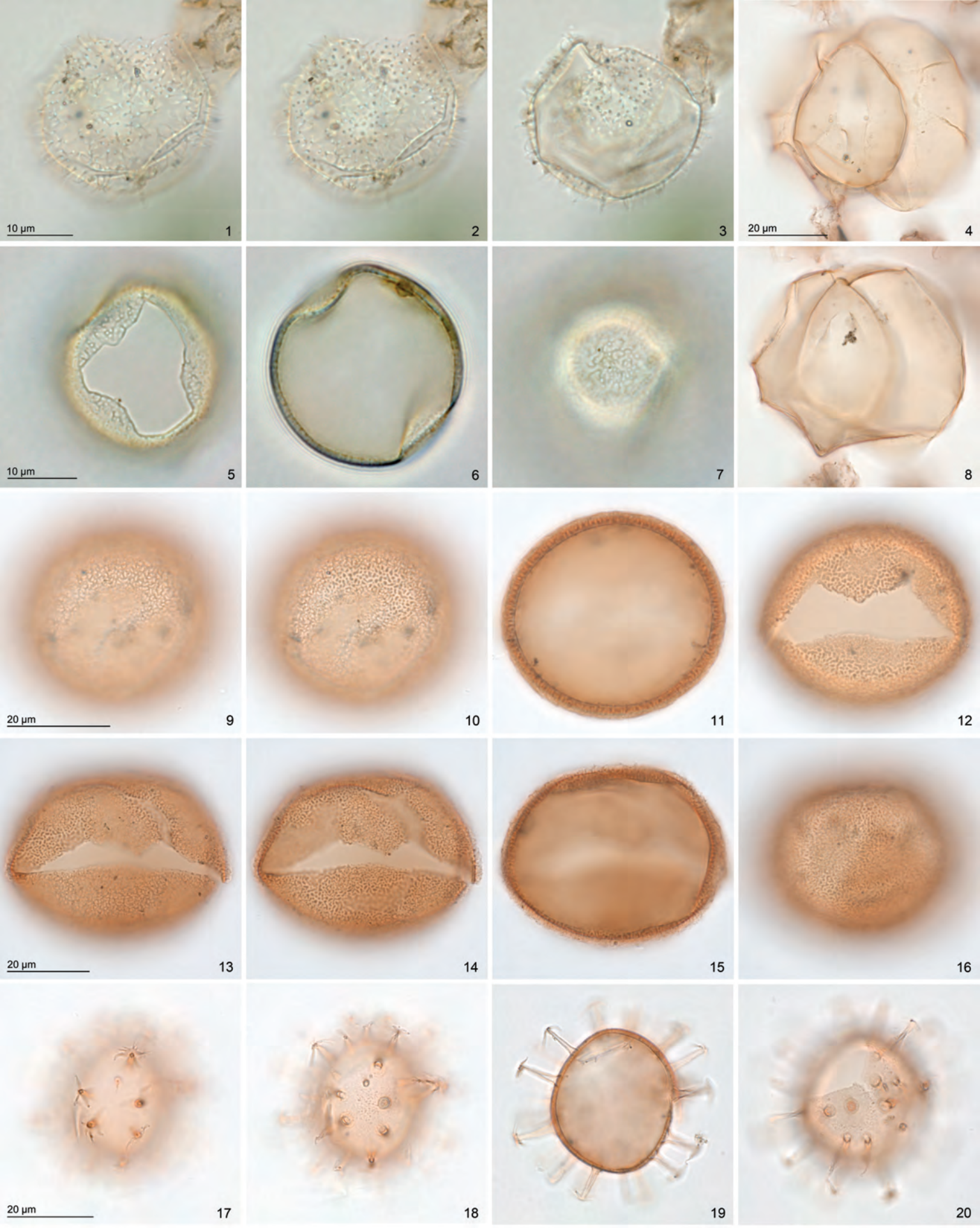
10 µm
1
2
3
20 µm
4
10 µm
5
6
7
8
20 µm
9
10
11
12
20 µm
13
14
15
16
20 µm
17
18
19
20

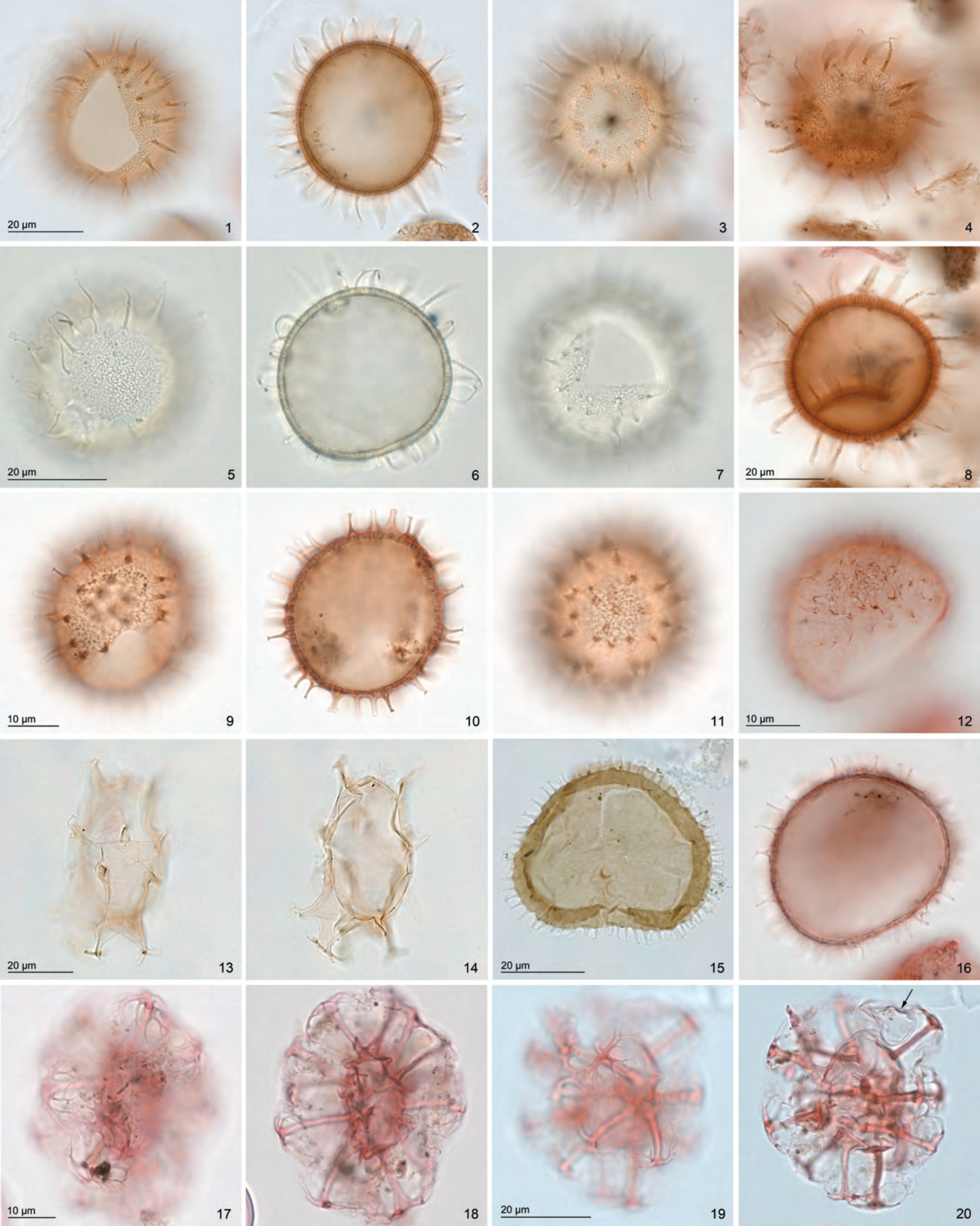
20 µm
1
2
3
4
20 µm
5
6
7
20 µm
8
10 µm
9
10
11
10 µm
12
20 µm
13
14
20 µm
15
16
10 µm
17
18
20 µm
19
20


10 µm
1
2
3
4
10 µm
5
6
7
20 µm
8
20 µm
9
10
11
20 µm
12
10 µm
13
14
20 µm
15
16
20 µm
17
18
10 µm
19
20

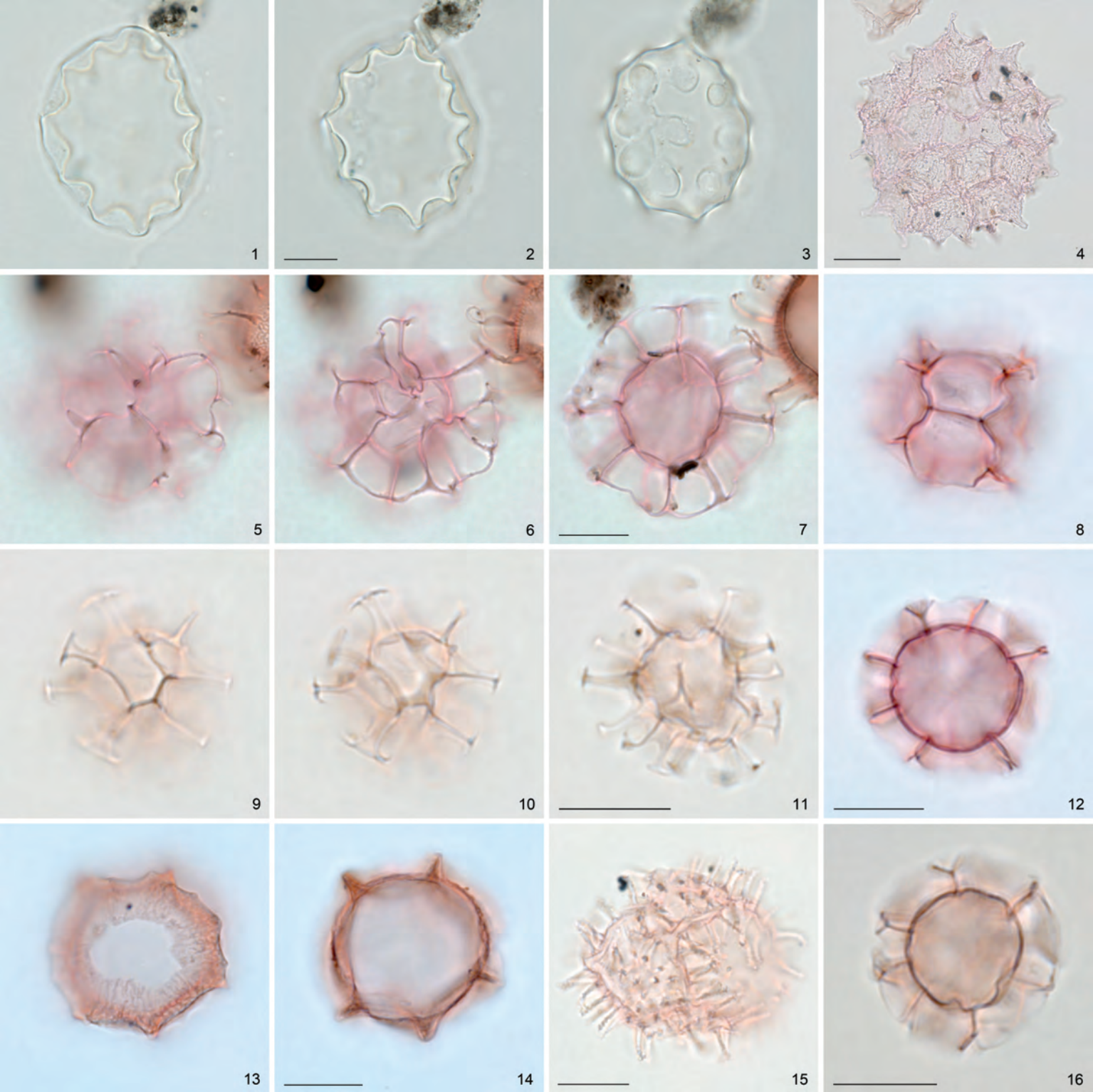
1
2
3
4
5
6
7
8
9
10
11
12
13
14
15
16

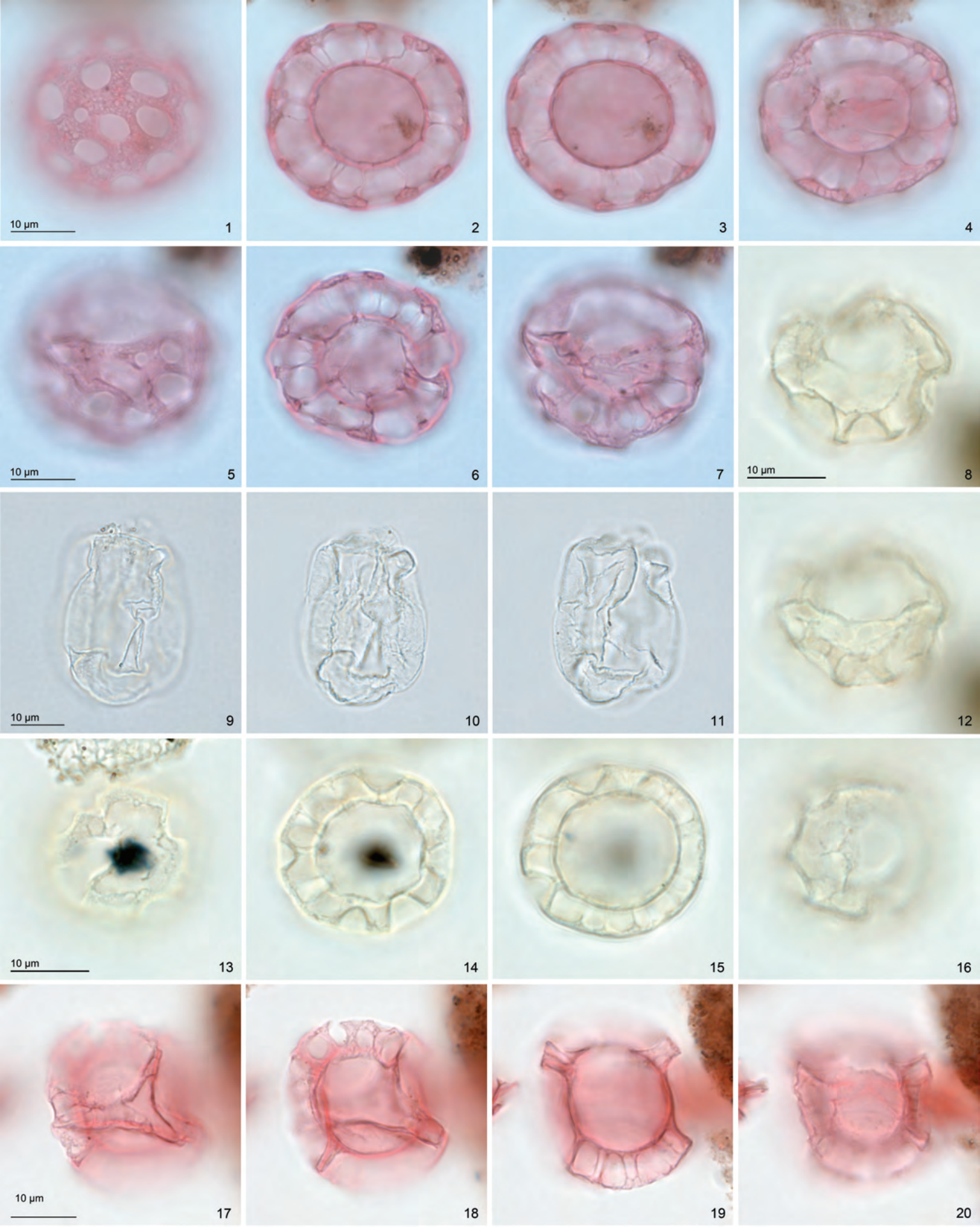
10 µm
1
2
3
4
5
6
7
10 µm
8
10 µm
9
10
11
12
10 µm
13
14
15
16
10 µm
17
18
19
20

Site	Hole	Core	Section	Interval (cm)	Depth (mbsf)	Calibrated ages (Ma)	Achomosphaera andalousiensis subsp. andalousiensis	Amiculosphaera umbraculum	Echinidinium spp. indet.	Habibacysta tectata	Impagidinium paradoxum	Lejeunecysta spp. indet.	Lingulodinium machaerophorum	Nematosphaeropsis labyrinthus	Operculodinium centrocarpum/israelianum	Operculodinium? eirikianum eirikianum	Round brown cyst	Spiniferites membranaceus	Spiniferites/Achomosphaera spp. indet.	Dinocyst spp. indet.	Barssidinium pliocenicum	Bitectatodinium sp. A	Invertocysta/Amiculosphaera spp. indet.	Impagidinium aculeatum	Impagidinium spp. indet.	Impagidinium pallidum	Pyxidinopsis braboi	Spiniferites mirabilis/hyperacanthus	Operculodinium sp. 1 of Louwye et al. (2004)	Filisphaera filifera subsp. pilosa	cysts of Protoceratium reticulatum	Bitectatodinium raedwaldii	Filisphaera filifera subsp. filifera	Filisphaera microornata
ODP 642	B	8	6	14–15	64.54	2.96	1	2	1	4	8	+	3	95	17	3	7	+	59	24	+	11	1	2	7	29	19	1	+	1	64	8	7	2
ODP 642	B	8	6	94–95	65.34	3.04			1	12		4	1	8	12	6	15			51		15	4	2	5	4	4	1			70	5	6	1
ODP 642	B	8	6	129–130	65.69	3.20–3.04	1	8		14			4	5	0	43			48	39		12		4		6			3		131	8	19	
ODP 642	B	9	1	50–51	66.90	3.20		1		250	1		+	26	19		1		82	27		15	1		3	1		+			34	4	20	
ODP 642	B	9	1	120–121	67.60	3.27	6	4		77	1		+	3	3		7		48	14	1	3		1	1	4	7			6	41	11	76	
ODP 642	B	9	2	20–21	68.10	3.32	1	4	1		2		3	9	1	2	3		63	9	2	7		1	6	14	22				114	8	9	
ODP 642	B	9	2	40–41	68.30	3.35	5	3		2	5		2	29	3	+	+	1	62	12		1		+	2	7	5	1			126	2	24	1
ODP 642	B	9	2	65–66	68.55	3.39	2	1		10	2		4	32	1	4	2	+	64	10		4		3	5	4	9			2	127	5	30	
ODP 642	B	9	2	110-111	69.00	3.45		1	1	+	4		24	30	2	13			100	13		13	1	7	1	10	14	+			206	6	20	
ODP 642	B	9	2	120–121	69.10	3.47		2		2	2		44	15	4	6	2		78	5	1	6		6	1	5	9	1			122	5	3	
ODP 642	B	9	3	55–56	69.95	3.59	1	2	5		6		17	22	2	84	6		131	8	+	4	4	3	6	8	4	1	+	3	158	1	5	
ODP 642	B	9	3	60–61	70.00	3.60		3		1	3		3	19	+	21	5	+	60	6	1	+		3		8	9	+	1	+	136	2	2	
ODP 642	B	9	3	70–71	70.10	3.61	+		1	1	+		7	30	+	32	16	1	50	8	2	4		2	4	11	8	6	1		97		1	
ODP 642	B	9	3	100–101	70.40	3.64	1	2			6		12	18	4	35	1	+	154	10		4	3		4	3	4		1	8	125		+	
ODP 642	B	9	3	105–106	70.45	3.64	+	6		2			8	10	1	12	+		130	8				2	3	13	28	3			144	8	4	
ODP 642	B	9	4	145–146	72.35	3.83	1	15	+	+	3			73	4	3	16		42	16	1	22	4	5		5	15	+	+	1	118	5	34	10
ODP 642	B	9	5	100–101	73.40	3.93	1	7	1	+	6	+	+	50	3	9	6		61	9	+	15	7	+	3	6	4	+		2	190		13	
ODP 642	B	9	6	100–101	74.90	4.08	2	+	+		3		+	23	1	6	7	4	51	14		9		3		9					80	5	36	2
ODP 642	B	9	7	11–12	75.51	4.14	1	+	+		3			20	3	16	17		84	15	+	7	2	7	12	21				5	140		16	
ODP 642	B	10	1	40–41	76.30	4.23	2		+	6	7		1	24	1	21	11		62	4	+	5	1	+		2	+	+	+	7	125	3	3	
ODP 642	B	10	1	145–146	77.35	4.49	3	+		+	6		5	24	57	32		1	73	8				2		3		+			17			
ODP 642	B	10	2	40–41	77.80	4.64	3	2			1	2	2	37	6	33	18		170	2	+	3	1	1	4	4					19		+	
ODP 642	B	10	2	100–101	78.40	4.69	2	+	+	+		3	1	28	2	23	29		151	11	+			1	1	7	4	+			3	3	1	
ODP 642	B	10	3	102–103	79.92	4.81	3		1	+	2	+		67	14	35	20		107	5	4	2		1		5			+			3	1	
ODP 642	B	10	4	15–16	80.55	4.84	2	1	5	1	2	5	1	162	22	36	89		97		+			1		4				3		1	7	
ODP 642	B	10	5	11–12	82.01	4.91			1			3		5	2	8	155		15	14		20		1		1				1			22	
ODP 642	B	10	5	115–116	83.05	4.98	+	2	+		1	3	2	12	48	52	15		56	7	+		+			2						6	+	
ODP 642	B	10	6	65–66	84.05	5.18	+	2	1		1	3	3	8	9	27	7	1	100	27	10				2	2	1	34		+		1	2	
ODP 642	B	10	7	30–31	85.20	5.29		1	2	7	1	2		35	25	54	18	+	51	6	2				2									
ODP 642	B	11	1	80–81	86.20	5.35		+	9	9	5	4	+	13	28	68	29	+	156		6		4		3	3								
ODP 642	B	11	2	15–16	87.05	5.41			8	10	4	5		36	10	35	35		151	7	2		1			2								
ODP 642	B	11	2	65–66	87.55	5.44			10	5	6	1	+	52	16	26	4		276	6	1	1	8		1						2			
ODP 642	B	11	3	65–66	89.05	5.53	4	1	28	11	+	10	3	34	23	17	70	+	136	4	+			1	1		+			1	+			
ODP 642	B	11	4	70–71	90.60	5.62	+		21	6	+	5	2	23	+	37	221		88	14	+					2			+					
ODP 642	B	11	5	60–61	92.00	5.71			4	8	6	3	1	37	4	35	12		212			1		+	4			+						
ODP 642	B	11	6	20–21	93.10	5.78	2		10	7	+	4	1	41	4	26	56		90	12	+	+	+	2	2	+	1							
ODP 642	B	11	6	70–71	93.60	5.81	1		41	4	1	1	+	5	+	5	204		30	20			+	1	4									
ODP 642	B	11	6	110–111	94.00	5.83	1			5		1	13	10	14	25	46		122	14	+	3												
ODP 642	B	11	7	15–16	94.55	5.87	3		2	17	+	1	2	120	6	35	40	+	130	26	+	+	2											
ODP 642	B	11	7	55–56	94.95	5.89	4	1	5	13	+	4	1	76	10	17	22	+	170	16														

Depth (mbsf)	Barssidinium graminosum	Pyxidinopsis spp.	Tectatodinium pellitum	Melitasphaeridium cf. choanophorum	Hystrichokolpoma rigaudiae	Impagidinium sp. 2 of De Schepper and Head (2009)	Filisphaera spp. indet.	Bitectatodinium? serratum	Invertocysta lacrymosa	Melitasphaeridium choanophorum	Nematosphaeropsis lativittata	Cyst of Pentapharsodinium dalei	Ataxiodinium zevenboomii	Corrudinium? labradori	Heteraulacacysta sp. A of Costa and Dowie (1979)	Corrudinium harlandii	Bitectatodinium tepikiense	Operculodinium janduchenei	Trinovantedinium glorianum	Ataxiodinium choane	Achomosphaera andalousiensis subsp. suttonensis	Desotodinium wrennii	Brigantedinium spp. indet.	Dapsilidinium pseudocolligerum	Selenopemphix dionaeacysta	Selenopemphix spp. indet.	Bitectatodinium spp. indet.	Nematosphaeropsis spp. indet.	Spiniferites sp. A of Louwye and De Schepper (2010)	Spiniferites elongatus	Ataxiodinium confusum	Impagidinium patulum	Tuberculodinium vancampoae	Operculodinium? eirikianum var. crebrum	Melitasphaeridium sp. A of De Schepper and Head (2008)
64.54																																			
65.34	1	+	1	4																															
65.69					1	2	1																												
66.90			1																																
67.60			+					2	2	1	1	1	1	1	6	2	1																		
68.10			1				2		+	3				1	15		3	1	2	1	1	+													
68.30	2		2	1	+				+	3		2		2	+	+		+		2			+	1	1	+	1	1	+	1					
68.55			1						9	1	1	3		2			1	+						+		1				1	1				
69.00	1		+						2	3		35		2	+	+		2		2			2	+			+			6	1	+	13	+	+
69.10		1							6	1		6		1	40					1					1	1				11					2
69.95	3							1	2			3	+	+	+			1	1						1					5		+		2	+
70.00	+				+	2	+	1	+			6		1	4	+		+	2	1	1		2		2	4			+	+	1	1		2	+
70.10			1				6		5			5		2	7	2	1	1		1						+				2	+	+		2	+
70.40									2	2		8		1			20			1												4		2	
70.45			1						6	1		2	1	2		3	34			1												3		29	
72.35	+		2			7		3	+	3		3		3		2	4	2	+	+	+		8	+	2		1		+	1				6	
73.40	+		+						1	1		26		2	+					+	1											+			
74.90			+			1		1	+	1		15		1		1				1									2			1			
75.51	1		+							2		29	1	+		1		+		2					+					1		1			
76.30	2		+			2			1	+		4	1	1		2		1	+	2			+	1								+		+	
77.35			1			2		+	1	2				3																	+	9			
77.80	15		+	4	+			+	7				1	7		1																+			
78.40	+							+	4	2		5	2	8	+					+	1		4		+	3	1		1						
79.92			+			1		3	1	2		16	+	20															11			+			
80.55	9								1	1			2	16					+				14		2	2			1			+			
82.01	1								1	3		1		2									8			6						1			
83.05	+		+						9	16		+	1	4									3		+				1			+			
84.05	7								2	2				+									4		5	1						3			
85.20									2	7					2				1							36	1					25	+		
86.20	+	+	2						12	4	1			+				+	+				2	1	5	29		16				11			
87.05	4		+						4	1			1					+	+	1					34	15						4			
87.55	13		3						+	3									+				2	1	5	16						2			
89.05	+		1		+				1	1		2							4				2	+	41	28			+			5			
90.60	5								1	4		2							8				5		17	10	3					+			
92.00	1		+		+			1	2	3				+					2						34	15						1			
93.10	2		+						+	3	+		1	+					20						59	19						2			
93.60	4		+					1		1									14				2		19	13	+					+			
94.00	+		5					2	1	4		2						2	1	+			8		13	5		15	2			+	+		
94.55		2	2						3	9								+					+	2	3	6	1					1			
94.95	2	+	1					2	4	4	1							+	+				+	1	6	8						8	+		

Depth (mbsf)	Selenopemphix nephroides	Impagidinium solidum	Lejeunecysta hatterasensis	Trinovantedinium variabile	Operculodinium spp. indet.	Invertocysta tabulata	Barssidinium sp. indet	Cerebrocysta? namocensis	Batiacasphaera/Pyxidinopsis spp. indet.	Impagidinium sp. 1 of De Schepper and Head (2009)	Corrudinium devernaliae	Operculodinium tegillatum	Invertocysta sp. I of de Vernal and Mudie (1989)	Batiacasphaera micropapillata complex	Reticulatosphaera actinocoronata	Selenopemphix brevispinosa	Cyst type 1 of de Vernal and Mudie (1989)	Ataxiodinium spp. Indet.	Batiacasphaera minuta s.s.	Selenopemphix quanta	Cristadinium diminutivum	Lejeunecysta catomus	Pyxidinopsis vesiculata	Batiacasphaera hirsuta	"Impagidinium densiverrucosum" of Zevenboom and Santarelli in Zevenboom (1995)	Impagidinium sphaericum	Cerebrocysta poulsenii	Selenopemphix armageddonensis	Labyrinthodinium truncatum	Pyxidinopsis sp. A	Trinovantedinium spp.	Batiacapshaera sphaerica	Biozones
64.54																																	Not zoned
65.34															1																		
65.69																																	
66.90																																	
67.60																																	VP3
68.10														1																			
68.30														1	+	+																	
68.55																																	
69.00																																	
69.10																																	
69.95	1	+																															
70.00	+																																
70.10	2		+	1																													
70.40																																	
70.45					4										1																		
72.35	1	+				+	1	1				1		2	+																		
73.40															1																		
74.90																																	
75.51									1																								
76.30									4	+						+																	
77.35					4						15	51	5																				
77.80	+								1		4	36		14	7	3	174																VP2
78.40	+										3	15		64	4	1	72	1															
79.92					7						2	41		41	12	5	3		+	+													
80.55	+										9	22		35	7	+			+														
82.01					1				1			13		28	7		1		+		2	+	1										
83.05	+											6		195	3	7			+		2?		+	1									
84.05	1					1						42			11	2			12														
85.20									4			2			4	3			7				5		1	13							VP1
86.20	10					+								7	19	4			1					2	4		1						
87.05	8		1				+		8		11				44	20									1			+	+				
87.55									9						19	11									1								
89.05	+		2		+	+			2		+				26	5			2			+		11	2					5			
90.60	2		+											16	15	5					1			8	1				+	1			
92.00														6	21	2		1				+		2	3					19			
93.10	2		+		+				4					14	15									8	1			1		4	8		
93.60	1		2		+									8	9				1		15			7	1				+	1	28		
94.00	+								7	2				10	8	1								3	2					34		1	
94.55	+				+				16					9	25	10			4		3			2	+		+			30	1		
94.95	2								5						20	6			6		1			1	3		+	+		13	2		

Site	Hole	Core	Section	Interval (cm)	Depth (mbsf)	Calibrated ages (Ma)	Cymatiosphaera? invaginata	Small spiny acritarchs	Nannobarbophora walldalei	**Cymatiosphaera? aegirii**	**Cymatiosphaera? icenorum**	Acritarchs spp. indet.	Cymatiosphaera spp. indet.	**Lavradosphaera crista**	**Cymatiosphaera? fensomei**	Lavradosphaera sp. cf. canalis	Lavradosphaera spp. indet.	**Lavradosphaera lucifer**	Acritarch sp. 1 of Head, Norris & Mudie (1989)	**"Veriplicidium franklinii" in Anstey (1992)**	Leiosphaeridia rockhallensis?	Cyclopsiella granosa	**Lavradosphaera canalis**	Lavradosphaera sp. 2 of Schreck et al. (2013)	**Biozones**
ODP 642	B	8	6	14–15	64.54	2.96	30	61	19	6	12			1											**Not zoned**
ODP 642	B	8	6	94–95	65.34	3.04	7	79	4																
ODP 642	B	8	6	129–130	65.69	3.20–3.04	10	17	53	3	1	6	4												
ODP 642	B	9	1	50–51	66.90	3.20	1	17	2																
ODP 642	B	9	1	120–121	67.60	3.27	16	87	16	2	17		12	8											**VP3**
ODP 642	B	9	2	20–21	68.10	3.32	23	58	1		4	1		16	1										
ODP 642	B	9	2	40–41	68.30	3.35	11	68	17		23	6		12											
ODP 642	B	9	2	65–66	68.55	3.39	+	35	1	2	1			3	+										
ODP 642	B	9	2	110-111	69.00	3.45	101	169	87	14	244			53											
ODP 642	B	9	2	120–121	69.10	3.47	60	50	57	11	93			41											
ODP 642	B	9	3	55–56	69.95	3.59	160	92	11	8	126			116		3									
ODP 642	B	9	3	60–61	70.00	3.60	277	87	15	28	256	13	1	228											
ODP 642	B	9	3	70–71	70.10	3.61	220	94	10	25	188			119	3										
ODP 642	B	9	3	100–101	70.40	3.64	4	81	38		3			1											
ODP 642	B	9	3	105–106	70.45	3.64		65	48	+	+														
ODP 642	B	9	4	145–146	72.35	3.83	128	492	20	19	768	8	2	158		+	1								
ODP 642	B	9	5	100–101	73.40	3.93	152	352	19	3	605			118											
ODP 642	B	9	6	100–101	74.90	4.08	590	995	27	18	459			341			2								
ODP 642	B	9	7	11–12	75.51	4.14	232	541	48	18	811			231											
ODP 642	B	10	1	40–41	76.30	4.23	184	494	31	7	245			223											
ODP 642	B	10	1	145–146	77.35	4.49	1																		
ODP 642	B	10	2	40–41	77.80	4.64	453	180	3		8			7											**VP2**
ODP 642	B	10	2	100–101	78.40	4.69	469	118	20		34	10		4			3	3							
ODP 642	B	10	3	102–103	79.92	4.81	216	144	12		25	3		13			3	6		+					
ODP 642	B	10	4	15–16	80.55	4.84	338	305	16		16		2	21				11							
ODP 642	B	10	5	11–12	82.01	4.91	1234	89	1		21	3	6	3	1			81	1						
ODP 642	B	10	5	115–116	83.05	4.98	144	37	8	1	1	4		26				41							
ODP 642	B	10	6	65–66	84.05	5.18	242	21	2			2	4	2				47							
ODP 642	B	10	7	30–31	85.20	5.29	49	14	1		2			12	1		1	6		7	1				**VP1**
ODP 642	B	11	1	80–81	86.20	5.35	100	95				+		8			3			59					
ODP 642	B	11	2	15–16	87.05	5.41	139	145	1	1	1			10						17					
ODP 642	B	11	2	65–66	87.55	5.44	19	132		2		7					3			23					
ODP 642	B	11	3	65–66	89.05	5.53	128	196	15	1	+			12					5	21					
ODP 642	B	11	4	70–71	90.60	5.62	48	123	1	1		+		6			+			13					
ODP 642	B	11	5	60–61	92.00	5.71	68	121				+	+	2			1			68		1			
ODP 642	B	11	6	20–21	93.10	5.78	205	166				3		4			6			13		+	10		
ODP 642	B	11	6	70–71	93.60	5.81	81	74						4			1			7			9		
ODP 642	B	11	6	110–111	94.00	5.83	104	169	19							3	7	4		4			1		
ODP 642	B	11	7	15–16	94.55	5.87	68	320				9		2		4	8	3		32			2		
ODP 642	B	11	7	55–56	94.95	5.89	30	235				7		7			1			16				1	